ESD-TR-76-63

See 1473

12

AD A024310

Project Report

TT-9

S. P. Tomczak

Diffuse Target Scintillation in 10.6 μm Laser Radar

8 March 1976

Prepared for the Defense Advanced Research Projects Agency
under Electronic Systems Division Contract F19628-76-C-0002 by

Lincoln Laboratory

MASSACHUSETTS INSTITUTE OF TECHNOLOGY

LEXINGTON, MASSACHUSETTS

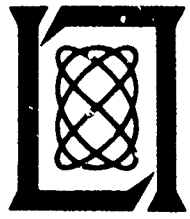

The work reported in this document was performed at Lincoln Laboratory, a center for research operated by Massachusetts Institute of Technology. This work was sponsored by the Defense Advanced Research Projects Agency under Air Force Contract F19628-76-C-0002 (ARPA Order 2752).

This technical report has been reviewed and is approved for publication.

FOR THE COMMANDER

Eugene C. Raabe

Eugene C. Raabe, Lt. Col., USAF
Chief, ESD Lincoln Laboratory Project Office

MASSACHUSETTS INSTITUTE OF TECHNOLOGY

LINCOLN LABORATORY

DIFFUSE TARGET SCINTILLATION IN 10.6 μm LASER RADAR

S. P. TOMCZAK

Group 53

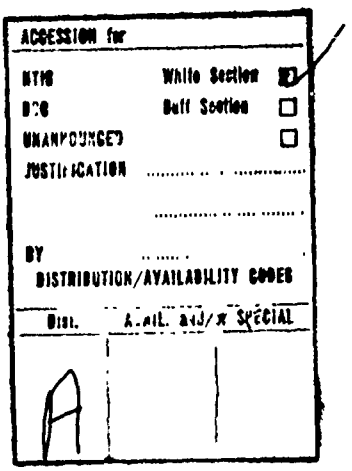

PROJECT REPORT TT-9

8 MARCH 1976

LEXINGTON MASSACHUSETTS

ABSTRACT

This study is concerned with effects of diffuse target scintillation on 10.6μm heterodyne line scan systems where the objective was to identify the problem areas which would eventually control the limiting factors in the image and MTI performance of line scan systems. In particular, diffuse target scintillation (speckle) was recognized as one of the limiting factors for a heterodyne receiver design and this study is concerned with the statistics of speckle noise and with speckle reduction techniques.

CONTENTS

LIST OF ILLUSTRATIONS

1. INTRODUCTION AND SUMMARY

The following report is a summary of the major topic of investigation for the laser line scanner study conducted for the HOWLS program from March 1, 1975 to August 1, 1975. The study is primarily concerned with effects of diffuse target scintillation of 10.6μm heterodyne line scan systems. An objective of this investigation was to identify the problem areas which would eventually control the limiting factors in the image and MTI performance of line scan systems. In particular, diffuse target scintillation (speckle) was recognized as one of the limiting factors for a heterodyne receiver design and the major emphasis of this report is concerned with the statistics of speckle noise and with speckle reduction techniques. Speckle reduction is especially important for heterodyne systems since, for single detector receivers, aperture averaging is not advantageous.

Coherent receiver technology has been developed to the point where the advantages of active coherent imagery and MTI have been clearly demonstrated. At 10.6μm these systems have qualitatively demonstrated the ability to obtain high resolution imagery, pointing and tracking, ranging, and doppler capability. However, quantitative data on the ultimate performance of coherent systems is scarce and there are many design areas which are in need of a quantitative measurements program which would provide more information for future system design.

It has become clear that some of the limiting factors in active systems at 10.6μm are the scintillations from diffuse targets (speckle), specular targets (glint) and atmospheric turbulence. The fluctuating signals from

these phenomena raise image contrast and lower the system S/N, angular resolution, and target/MTI detection probabilities. In the report that follows we wish to outline a measurement program that would obtain quantitative data from laboratory measurements which would enhance future systems which are designed to reduce speckle.

We are concerned with the quality of coherent images obtained from an active line scanner system which operates at 10.6μm. We wish to obtain the maximum quantitative information from targets and backgrounds of known reflectivity and surface characteristics. In particular we wish to make known the relation between image contrast and angular resolution for coherent receivers in situations which the contrast is dominated by diffuse target scintillation.

The noise equivalent reflectivity of an active line scanner is the minimum difference in reflectivity observed and is limited by the system noise or target scintillation. It will be shown that the background and targets diffuse surface qualities can introduce an associated noise that is equivalent to an RMS uncertainty in the measured reflectivity differences of 100%. Clearly, imaging and MTI systems cannot operate under these circumstances and means must be found to reduce this target noise.

It will be shown that for case where the diffuse signal dominates the specular component the signal amplitude will obey Rayliegh statistics while the intensity follows an exponential distribution. When a specular signal is present with the diffuse component, we will show the intensity follows a modified Rayliegh or a Rician distribution. In particular, it will be shown

that the specular component's signal to noise ratio will modify the noise spectrum and control the moments of the probability distribution. The point that we wish to emphasize is that the specular and diffuse components are not independent and the moments of the diffuse scintillation statistics depend on the presence of the specular component. In cases where the diffuse signal fluctuation is high and where incoherent addition of images is required it is found that the image improvement will depend on the signal to noise of the specular component.

The most straightforward way of improving the imagery is to obtain several images, each with its independent noise characteristics, and then incoherently add these images. In performing this addition the signal increases as the number of independent observations, N, while the RMS fluctuations increase as $\sqrt{N}$, and the image S/N improves as $\sqrt{N}$. Thus, if we had an image with a RMS fluctuation of 50% and we wish to reduce this fluctuation to 5% we would have to obtain 100 dependent images to gain a factor of 10 in the RMS signal fluctuation. If a system design or mission calls for a noise equivalent reflectivity difference of, say, .05, and if we expect a diffuse scintillation fluctuation of 50% we must determine the best way to obtain 100 dependent observations. It should be emphasized that a large power S/N is not required for each independent observation and this fact will be of great assistance in the system design when available transmitter powers are restricted to low values.

Another point to be emphasized is that in order to obtain images with independent noise fluctuations the target and receiver should not introduce

correlations between observations. In the sections that follow we will describe target scintillation averaging techniques in which the measurements are believed to have correlated statistics. It will be necessary to perform measurements with diffuse bar charts to demonstrate that the frames obtained are indeed independent and that an improvement in the image S/N increases as the square root of the number of independent observations.

When diffuse scintillation reduction is necessary it will be required to combine images with independent noise statistics. The independence of the noise statistics will depend on the amplitude spatial correlation at the receiver aperture. The theory of this correlation is presented and an equation for the amplitude correlation distance is derived.

We then discuss various methods used to reduce diffuse target scintillation which include: multiple observations, multiple receiver and transmitter averages, focal plane arrays, polarization averaging, and frequency averaging. A derivation of the origin of the wavelength dependence of the diffuse scintillation is also presented.

Finally we discuss methods whereby the speckle reduction can be observed in the laboratory. In particular, the system noise equivalent reflectivity and angular resolution degradation can be observed by employing diffuse bar charts of known surface characteristics. From these measurements the moments of the scintillation can be measured and the decorrelated images can be combined to observe the reduction in noise.

The author would like to thank Dr. David Fried, OSC, Prof. Nicholas George, C.I.T., and Prof. Joseph Goodman, Stanford University for the many

helpful discussion concerning the topics discussed in this report. Special thanks go to Harvey Buss, Lincoln Laboratory, for his assistance with the calculations.

2. AMPLITUDE CORRELATION DISTANCE

An intuitive description for the origin of diffuse target scintillation may be obtained from the following argument. Figure 1 shows a plane wave falling on a diffuse reflector with diameter L_{Targ}. The diffuse surface will introduce a random phase shift across the target and in the far field a spatially modulated field pattern will be observed. The origin of this spatial modulation is the randomly phase shifted Huygen wavelets emanating from the illuminated surface. As the transmitted beam is scanned across the diffuse surface the spatial modulation of the far field constantly changes and the receiver will find maxima and minima in a random fashion. The end result is an image with a highly granular appearance with a low information signal to noise and a degraded angular resolution. The statistics of the fluctuations will be described and it will be shown that the RMS fluctuation can be as large as the signal mean. This can yield close to 100% noise in cases where there are small changes in reflectivity.

In order to perform diffuse target scintillation reduction through the incoherent additions of images with independent signal fluctuations, we need to obtain the size of the diffuse target correlation length L_C. Consider the arrangement in Figure 1. The diffuse target correlation length is the distance required in moving the receiver aperture from point P_1 to

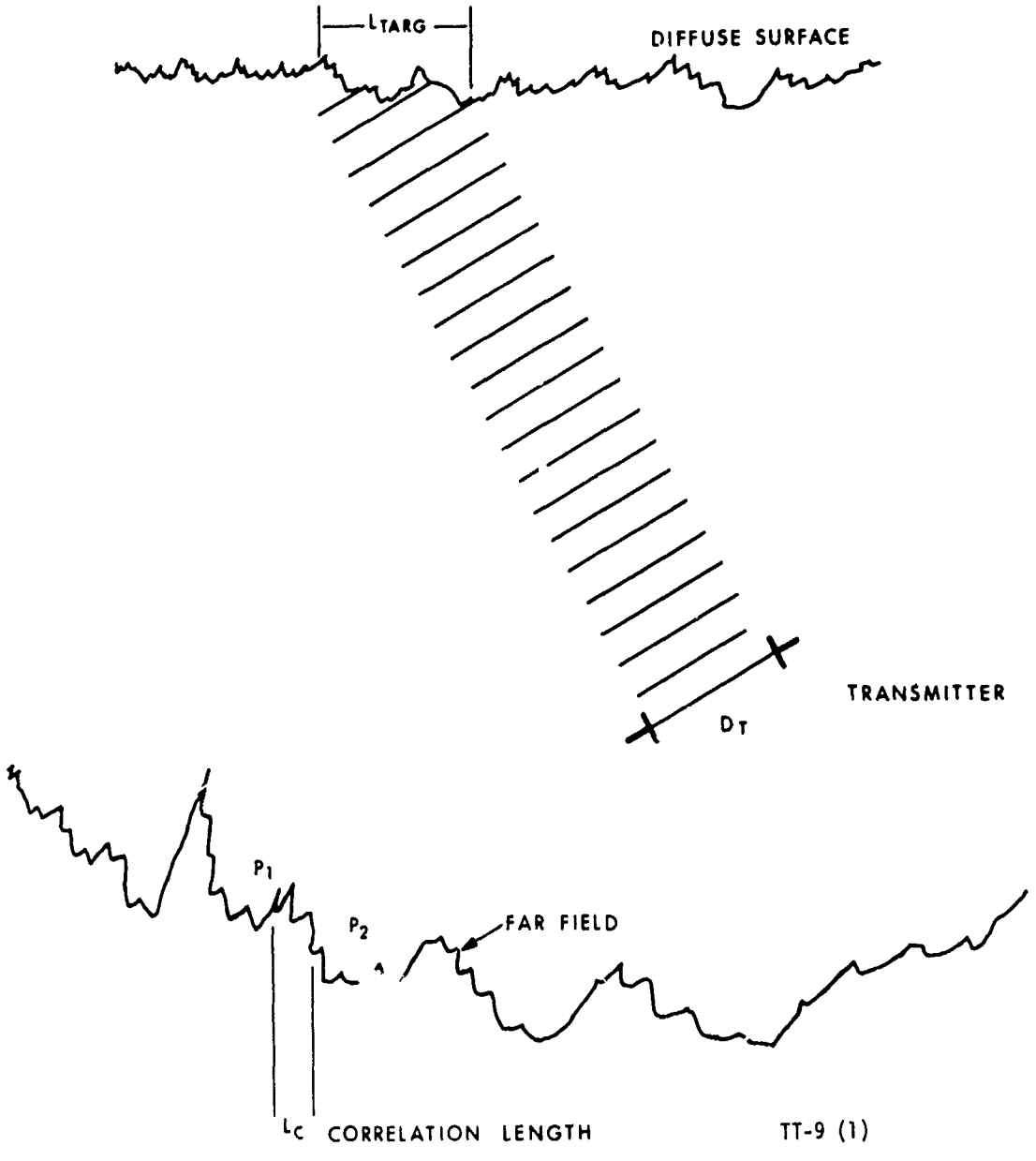

Fig. 1. A plane wave across a diffuse surface creates a far field pattern with a spatial amplitude correlation length L_C.

P_2 to obtain a signal at point P_2 uncorrelated with that signal at P_1. The correlation length may be obtained by recognizing that it is the separation required to have the amplitude at points 1 and 2 uncorrelated.

The amplitude correlation distance may be obtained directly if one treats the illuminated target as a spatially incoherent source which is certainly valid for a diffuse surface with a large number of scatterers. We will show that the phase correlation distance L_C is given by

$$L_C \cong R \frac{\lambda}{L_{Targ}}$$

where R is the distance from the target to the position midway to points 1 and 2. To obtain the correlation distance, we refer to Figure 2 where the source is a laser illuminated spot which we assume to be a diffuse surface. For simplicity, we imagine that the diffuse source is a collection of N independent scatterers and we wish to obtain the amplitude correlation at the points P_1 and P_2 in Figure 2. $A_i^{(1)}$ is the complex amplitude at the point P_1 associated with the i^{th} scatterer.

The total amplitude at P_1 is given by

$$A^{(1)} = \sum_{i=1}^{N} A_i^{(1)} = \sum_{i=1}^{N} \sqrt{I_i}\, e^{\,i\,k\,R_i^{(1)}}$$

where I_i is the average intensity of the i^{th} scatterer and $R_i^{(1)}$ is its range to the point P_1 shown in Figure 2.

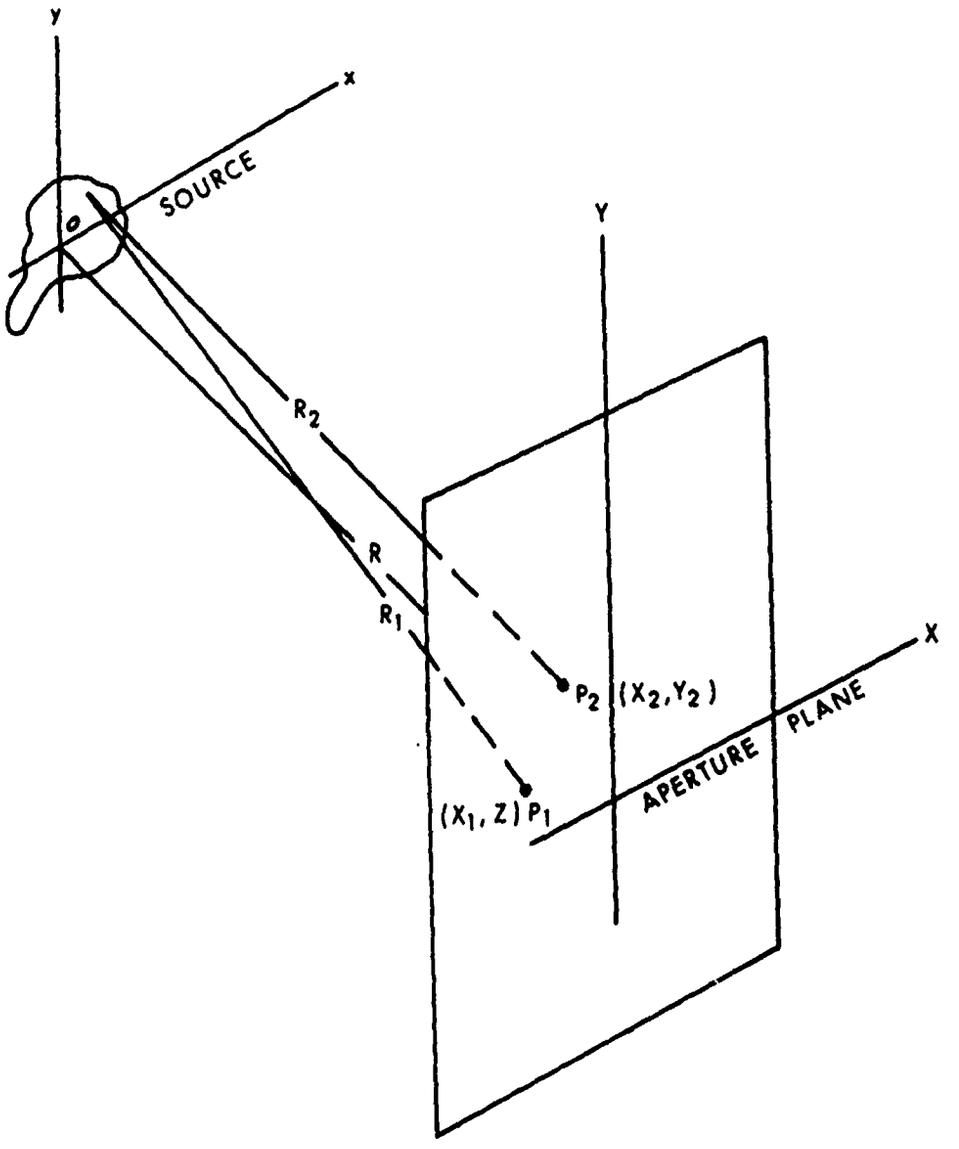

Fig. 2. The geometry for a diffuse source in the plane (x,y) and a receiver plane (X,Y) at a range R.

and the complex amplitude correlation function is given by

$$\overline{A^{(1)}\, A^{(2)*}} = \sum_{i,j=1}^{N} \overline{A_i^{(1)}\, A_j^{(2)*}}$$

$$= \sum_{i=1}^{N} \overline{A_i^{(1)}\, A_i^{(2)*}} + \sum_{i \neq j}^{N} \overline{A_i^{(1)}\, A_j^{(2)*}}$$

where the bars denote an ensemble average.

We now employ our assumption of a diffuse source which implies that the N scatterers are independently oriented and so large in number that

$$\sum_{i \neq j}^{N} \overline{A_i^{(1)}\, A_j^{(2)*}} = 0, \; i \neq j$$

and the amplitude correlation function simplifies to

$$\overline{A^{(1)}\, A^{(2)*}} = \sum_{i=1}^{N} \overline{A_i^{(1)}\, A_i^{(2)*}}$$

$$= \sum_{i=1}^{N} I_i \exp\left[i k \left(R_i^{(1)} - R_i^{(2)}\right)\right]$$

If $I(\sigma)\, d\sigma$ is the intensity from differential area $d\sigma$ the correlation function may be written

$$\overline{A_1(P_1)\, A_2^{*}(P_2)} = \int_S I(\sigma) e^{ik(R_1 - R_2)}\, d\sigma$$

and we wil' now show that this reduces to the form

$$\overline{A_1\,(P_1)\,A_2^{*}\,(P_2)} = \int\int_S I\,(x,y)e^{-ik(px+qy)}\,dx\,dy$$

where we follow Born and Wolf[1] with

$$p = \frac{\bar{X}_1 - \bar{X}_2}{R}\,, \quad q = \frac{\bar{Y}_1 - \bar{Y}_2}{R}$$

with R_1, R_2, $\bar{X}_1$, and $\bar{Y}_1$ shown in Figure 2.

Now with (x,y) the source coordinates and $(\bar{X}_1,\bar{Y}_1)$ and $(\bar{X}_2,\bar{Y}_2)$ as shown we have

$$R_1^2 = (\bar{X}_1 - x)^2 + (\bar{Y}_1 - y) + R^2$$

$$R_1 \cong R + \frac{(\bar{X}_1 - x)^2 + (\bar{Y}_1 - y)^2}{2R}$$

with similar equations for R_2^2 and R_2 since $\bar{X}_1/R$, x/R, and y/R are all much less than unity. The difference in P_1 and P_2 is

$$R_1 - R_2 \cong \frac{(\bar{X}_1^2 + \bar{Y}_1^2) - (\bar{X}_2^2 + \bar{Y}_2^2)}{2R}$$

$$- \frac{(\bar{X}_1 - \bar{X}_2)x + (Y_1 - Y_2)y}{R}$$

and substituting for p and q we have

$$R_1 - R_2 = \frac{(\bar{X}_1^2 + \bar{Y}_1^2) - (\bar{X}_2^2 + \bar{Y}_2^2)}{2R}$$

$$- px + qy$$

and we write the correlation function as

$$\overline{A_1 (P_1) A_2 * (P_2)} = \exp (i\psi)x$$

$$\int_S \int dxdy\ I (x,y) \exp (-ik(px + qy)$$

where

$$\psi = \frac{k[(\bar{X}_1^2 + \bar{Y}_1^2) - (\bar{X}_2^2 + \bar{Y}_2^2)]}{2R}$$

represents the phase difference $2\pi\ (O'P_1 - O'P_2)\ /\lambda$ and is usually neglected since

$$2\pi k(O'P_1 - O'P_2) << \pi$$

and we obtain

$$\overline{A_1 (P_1) A_2 * (P_2)} = \int \int dxdy\ I (x,y)$$

$$x \exp (ik(px + qy))$$

and if the source is a disk with radius ρ and $I(x,y) = I_o$ we obtain

$$\overline{A_1(P_1)\, A_2^*(P_2)} = \frac{2I_o J_1(\nu)}{\nu}$$

where

$$\nu = \frac{k\rho}{R}\sqrt{(\bar{X}_1 - \bar{X}_2)^2 + (\bar{Y}_1 - \bar{Y}_2)^2}$$

$$= \frac{k\rho}{R}\,\Delta R$$

where the integration is the standard form found in diffraction theory. J_1 is the first order Bessel function of the first kind. This result was first obtained by van Cittert[1] and is the same pattern that one would obtain if the source was a diffraction aperture where the aperture now has an amplitude distribution which is given by the intensity across the source.

The spatial correlation length will be obtained when we employ the condition $\Delta R \sim L_C$ where $J_1(\nu) = 0$. We have

$$\frac{2\pi k\rho L_C}{R} = 1.2\pi$$

$$L_C \cong \frac{\lambda}{L_{Targ}} R$$

with $L_{Targ} = 2\rho$.

For cases where the target illumination spot is given by

$$L_{Targ} \cong R\,\theta_L$$

where θ_L is the transmitter divergence we obtain

$$L_C \cong \frac{\lambda}{\theta_L}$$

and for a diffraction limited transmitter, $\theta_L \cong \lambda/D_T$, we have

$$L_C \cong D_T$$

where D_T is the transmitter diameter.

In sections 5.1 and 5.2 we will discuss the spatial and angular averaging of images that contain diffuse target scintillation noise. We will see that the correlation distance $L_C \cong D_T$ will be employed in system design to obtain images whose noise probability distributions are independent.

3. WAVELENGTH DEPENDENCE

The origin of the speckle wavelength sensitivity is the coherence time of the light source. If a light source has a spectral density $S(\sigma)$ with an average width of $\Delta\sigma$ (wavenumber, cm^{-1}) then the temporal coherence time of the light is given by

$$\Delta t_C \sim \frac{1}{c\Delta\sigma}$$

where c is the velocity of light.

We say that the electromagnetic wave consists of wavepackets with a coherence length of $c\Delta t_c \sim \Delta\sigma^{-1}$. The physical interpretation of the coherence time is the temporal analog to spatial coherence and has its origin in the amplitude time correlation which occurs at one point is space. The Michelson interferometer spectrometer measures this time correlation (by introducing a time delay $\delta t = \delta x/c$ where δx is the mirror retardation) and records through the amplitude correlation function

$$\overline{A(t)\,A^{*}(t+\delta t)} = \overline{A(x/c)\,A^{*}(x/c+\delta x/c)}$$

where the bars denote an ensemble average. The Fourier transform of the interferogram, $\overline{A(t)\,A^{*}(t+\delta t)}$, gives the power spectrum of the field $S(\nu)$ which has a spectral width $\delta\nu$ (Hertz).

Now consider a plane wave of spectral width $\Delta\sigma$ falling on a diffuse source which has a mean roughness height ℓ_o. For simplicity, let us consider the two spectral patterns which originate from planes A + B shown in Figure 3. If the distance ℓ between planes A and B is much shorter than the temporal coherence length, i.e., $\ell \ll \Delta\sigma^{-1}$, then there will be a strong temporal phase correlation between the two patterns and the speckle pattern from each will be highly correlated. If however, $\ell \gg \Delta\sigma^{-1}$, the temporal phase correlation between the two planes will be lost and the speckle patterns will be independent. In this case, the patterns from plane A and B originated from wavelengths which were separated in time by $\delta t = \ell/c$ and this time separation was large enough to cause a phase

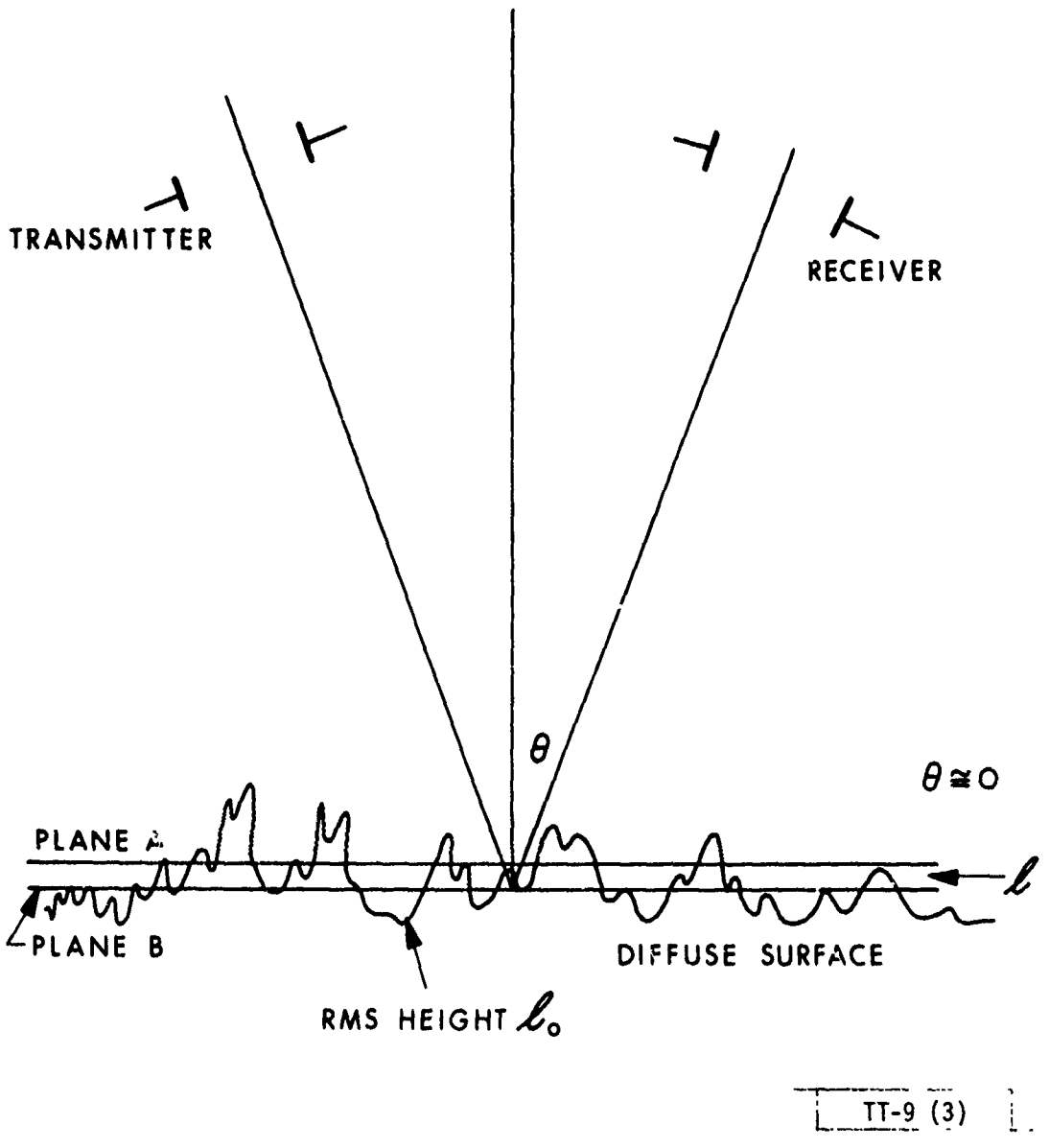

Fig. 3. The variation in height of the scatterers of a diffuse surface can contribute to diffuse target scintillation averaging for $\ell_o > \Delta\sigma^{-1}$.

decorrelation in the wave.

We thus arrive at the following condition. If the RMS height variation ℓ_o of a diffuse source is such that

$$\ell_o << 2\pi \frac{\lambda^2}{\Delta\lambda}$$

the image will be highly speckled. Note we have written $\Delta\sigma = \Delta\lambda/\lambda^2$ where $\Delta\lambda$ is the width of the spectrum in microns.

In the model discussed in Figure 3 we have assumed that the laser radiation was normal to the planes A and B and that the necessary time delay was due to the separation distance ℓ. Speckle pattern decorrelation may also be obtained from the geometry shown in Figure 4 where the angle of incidence is given by the angle θ and the illuminated spot now takes the shape of an ellipse instead of a circle. Now consider the simplified case where the diffuse elliptical reflector consists of one diffuse plane in contrast to the dual plane source shown in Figure 3. Due to the fact that sections of the ellipse have a different range we can obtain independent speckle patterns from each elliptical cross section which satisfies the inequality.

$$\delta R > \frac{1}{\Delta\sigma}$$

where δR is shown in Figure 4 and is given by

$$\delta R = \frac{2r}{N \cos\theta}$$

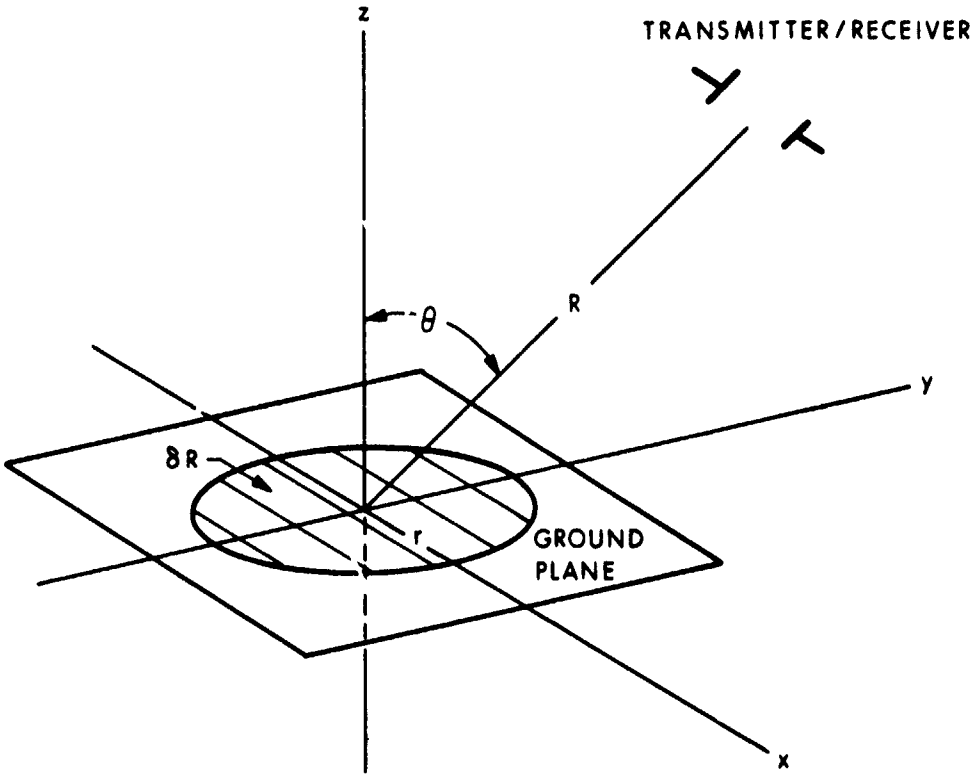

TT-9 (4)

Fig. 4. As in Figure 3, a variation in range of the scatterers of a diffuse surface can contribute to diffuse target scintillation averaging for $\delta R > \Delta\sigma^{-1}$.

where r is the spot radius at normal incidence and N is the number of independent strips in the distance $r\ (\cos\theta)^{-1}$. Thus, in order to have N independent speckle patterns from a frequency source with a spectral width $\Delta\sigma$ we must satisfy.

$$N < \Delta\sigma \frac{2r}{\cos\theta}$$

The methods to reduce the speckle contrast will be described in the section on frequency averaging.

The radius r along the χ axis in Figure 4 is given by

$$r = \frac{1}{2} R \cdot \theta_T$$

where R is the range and θ_T is the transmitter divergence and for a diffraction limited transmitter we have

$$r = R\lambda/2D_T$$

In this case the number of independent images that will be obtained is given by

$$N \leqq \Delta\sigma \cdot \frac{R\lambda}{D_T \cos\theta}$$

To obtain frequency averaging during the duration of one detector dwell time t_D the detector will have to observe N independent phase correlations in this interval.

That is,

$$Nt_c \lesssim t_D$$

and an upper limit on the number of independent distributions is given by

$$N = c\Delta\sigma\, t_D$$

Since for most CO_2 laser sources $\Delta\sigma$ is usually less than a wavenumber we will not obtain frequency averaging unless t_D is very long or frame to frame averaging is employed. In this case the dwell time is replaced by the image repeat time and N can be considerably increased.

4. DIFFUSE SCINTILLATION PROBABILITY DISTRIBUTIONS

4.1 No Specular Component Present

We consider the case of a plane wave falling on a diffuse target which consists of a very large number of scatterers. The complex amplitude is given by

$$\underline{A} = A_1 + i\, A_2$$

and the modulus by

$$A = (A_1^2 + A_2^2)^{1/2}$$

Each scatterer will introduce a random shift to the phase and in the limit of a very large number of scatterers we assume that the amplitude will be normally distributed. The joint probability density corresponding to the

real and imaginary parts of the field is given by

$$P(A_1, A_2) = \frac{1}{(2\pi\sigma^2)^{1/2}} \exp\left[-\frac{A_1^2 + A_2^2}{2\sigma^2}\right]$$

where σ^2 is the variance.

We wish to express this probability density in terms of the intensity and the phase. The statistics of these new variables are obtained from

$$I = A^2$$

$$= A_1^2 + A_2^2$$

which is the statistical variable which must be considered when dealing with a process such as square law detection. The statistics of the phase are also important and may be obtained from the change in variables

$$\phi = \tan^{-1}\left[\frac{A_2}{A_1}\right]$$

or

$$A_1 = I^{1/2} \cos\phi$$

$$A_2 = I^{1/2} \sin\phi$$

and the joint probability function of I and ϕ is then given by the transformation

$$P(A_1, A_2) = P(I^{1/2}\cos\phi, I^{1/2}\sin\phi)$$

and since the intensity and phase are independent we have

$$P(I, \phi) = P(I)\,P(\phi)$$

where a change to polar coordinates gives

$$P(I) = \frac{1}{2\sigma^2}\exp(-I/2\sigma^2),\ I \geq 0$$

$$= 0 \text{ otherwise}$$

and

$$P(\phi) = \frac{1}{2\pi} \quad 0 \leq \phi \leq 2\pi$$

$$= 0 \text{ otherwise}$$

Thus, when no specular component is present the intensity follows an exponential probability distribution while the phase is uniformly distributed. When a signal is present the intensity does not follow a negative exponential distribution and will be shown in a later section to follow a Rician distribution.

4.2 The Addition of Uncorrelated Intensity Distributions

We wish to obtain the new probability density which is obtained from the addition of M speckle patterns. We know that the i^{th} distribution follows

$$P_i(I_i) = \lambda_i^{-1} \exp(-I_i/\lambda_i),\ I > 0$$

$$= 0 \quad \text{otherwise}$$

where $\lambda_i = 2\sigma_i^2$ was seen to be the mean intensity.

The characteristic function corresponding to $p_i(I_i)$ is given by

$$C_i(\omega) = \frac{1}{1 - j\omega\lambda_i}$$

Since the distributions are independent[2]

$$C(\omega) = \prod_{i=1}^{M} C_i(\omega)$$

$$= \prod_{i=1}^{M} (1 - j\omega\lambda_i)^{-1}$$

and the new probability density is given by

$$P_M(I) = \int d\omega\, C(\omega)\, e^{j\omega I}$$

$$= \int \frac{d\omega e^{j\omega I}}{\prod_{i=1}^{M} (1 - j\omega\lambda_i)}$$

for $I \geq 0$ and zero otherwise.

Consider first the case where all the original probability distributions have the same mean intensity, i.e.,

$$\lambda = \lambda_1 = \lambda_2 = \ldots = \lambda_M = 2\sigma^2$$

We then obtain

$$P_M(I) = \int d\omega \frac{e^{j\omega I}}{(1 - j\omega\lambda)^M}$$

$$= \frac{I^{M-1}}{(M-1)!\ (\lambda)^M} \cdot \exp(-I/\lambda)$$

In terms of the normalized variable $x = I/\lambda$ we obtain

$$P_M(x) = \frac{1}{\Gamma(M)}\ x^{M-1}\ \exp(-x)$$

which is shown in Figure 5 for various values of M. The variance of this distribution is given by

$$\Delta^2 I = \frac{\bar{I}^2}{M}$$

and the contrast improves as the inverse square root of the numbers of independent observations. Note we have written $(M-1)! = \Gamma(M)$.

The moments of this Γ-distribution are given by

$$\overline{I_M^N} = \int_0^\infty dI\ I^N\ p_M(I)$$

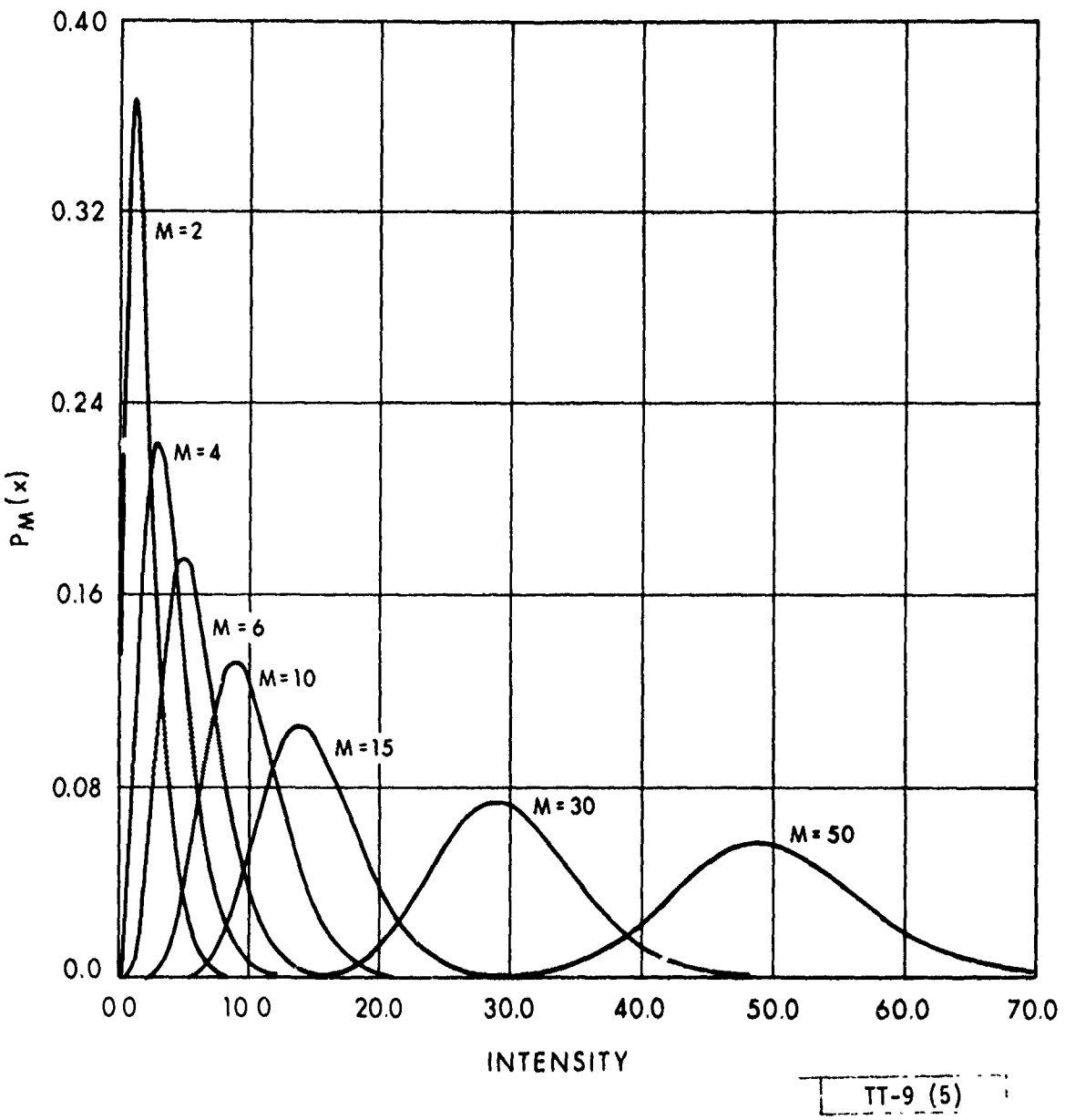

Fig. 5 The normalized intensity distribution for M equal variates with values shown for M = 2, 4, 6, 10, 15, 30, 50.

$$= \int_0^\infty dI \quad \frac{I^{M+N-1}\exp(-I/\lambda)}{(M-1)!\ (\lambda)^M}$$

$$= (\lambda)^N \quad \frac{(M+N-1)!}{(M-1)!}$$

for $\lambda_i = \lambda$, for $i = 1, \ldots, M$.

The first and second moments are given by

$$\overline{I}_M = 2\sigma^2 \cdot M$$

$$\overline{I_M^2} = 4\sigma^4\, M(M+1)$$

and the variance is

$$\overline{I_M^2} - \overline{I}_M^{\,2} = 4\sigma^4 M.$$

The mean square noise contrast is given by

$$C_I^{\,2}(M) = \frac{\overline{I_M^2} - \overline{I}_M^{\,2}}{\overline{I}_M^{\,2}} = \frac{1}{M}$$

and the root mean contrast is

$$C_I^{\,1/2}(M) = \frac{1}{\sqrt{M}}$$

which shows that for M uncorrelated patterns the mean noise contrast improves as we had earlier expected.

We now turn to the problem of M uncorrelated speckle distributions which differ in their mean intensities, i.e.,

$$\lambda_1 \neq \lambda_2 \neq \ldots \neq \lambda_M.$$

In this case the probability distribution is

$$P_M(I) = \sum_{i=1}^{M} \frac{\lambda_i^{M-2}}{\prod_{\substack{j=1 \\ j\neq i}}^{M} (\lambda_i - \lambda_j)} \exp(-I/\lambda_i)$$

The moments of this distribution are given by

$$\overline{I^N} = \sum_{i=1}^{M} \frac{\lambda_i^{M+N-1}}{\prod_{\substack{j=1 \\ j\neq i}}^{M} (\lambda_i - \lambda_j)}$$

We now take the special case where the mean intensity is given by

$$\lambda_i = \lambda_0 + i\Delta I$$

This will correspond to M independent distributions which can be arranged with average intensity differing by ΔI.

We then have

$$P_M(I) = \sum_{i=1}^{M} \frac{(\lambda_o + i\Delta I)^{M-2}}{\Delta I^{M-1} \prod_{i\neq j}^{M} (i-j)} \exp\left[-I/(\lambda_o + i\Delta I)\right]$$

which is shown in Figures 6-7 for various values of $\Delta\lambda$ and M.

The moments are given by

$$\overline{I^N} = \sum_{i=1}^{M} \frac{(\lambda_o + i\Delta I)^{M+N-1}}{(\Delta I)^{M-1} \prod_{\substack{j=1 \\ i\neq j}}^{M} (i-j)}$$

It should be pointed out that the probability distributions for the speckle pattern are expected to follow the distributions we have discussed but this remains to be observed experimentally. To observe the character of these distributions, a measurement of the higher order moments should be conducted. The higher order moments of single patterns should first be obtained and then these patterns should be combined and the process repeated. Before the individual patterns are combined, it should be verified that they are statistically uncorrelated. This should be accomplished by calculating the cross correlation coefficients $\overline{I_i I_j}$ for each position in the image. If a correlation is found, it should be determined if this is due to the presence of a signal by observing the spatial dependence of $\overline{I_i I_j}$.

4.3 The Addition of Uncorrelated Amplitude Distributions

So far we have been concerned with the addition of speckle intensity

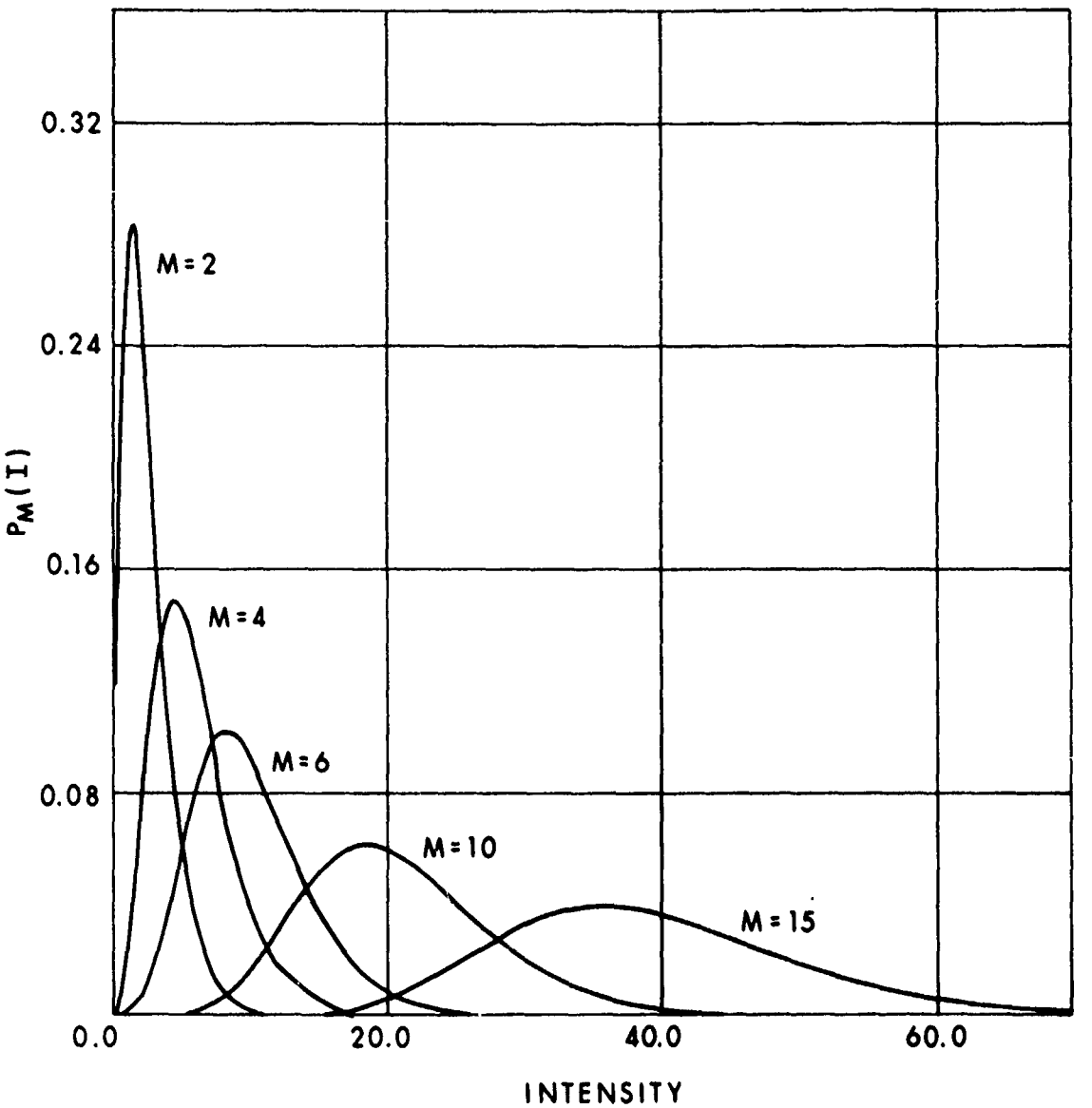

Fig. 6 The intensity probability distribution for M unequal variates with means satisfying $\lambda_1 = \lambda_0 + i\,\Delta\,I$, $i = 1,\ldots, M$. $\Delta I/\lambda_0 = .2$

TT-9 (7)

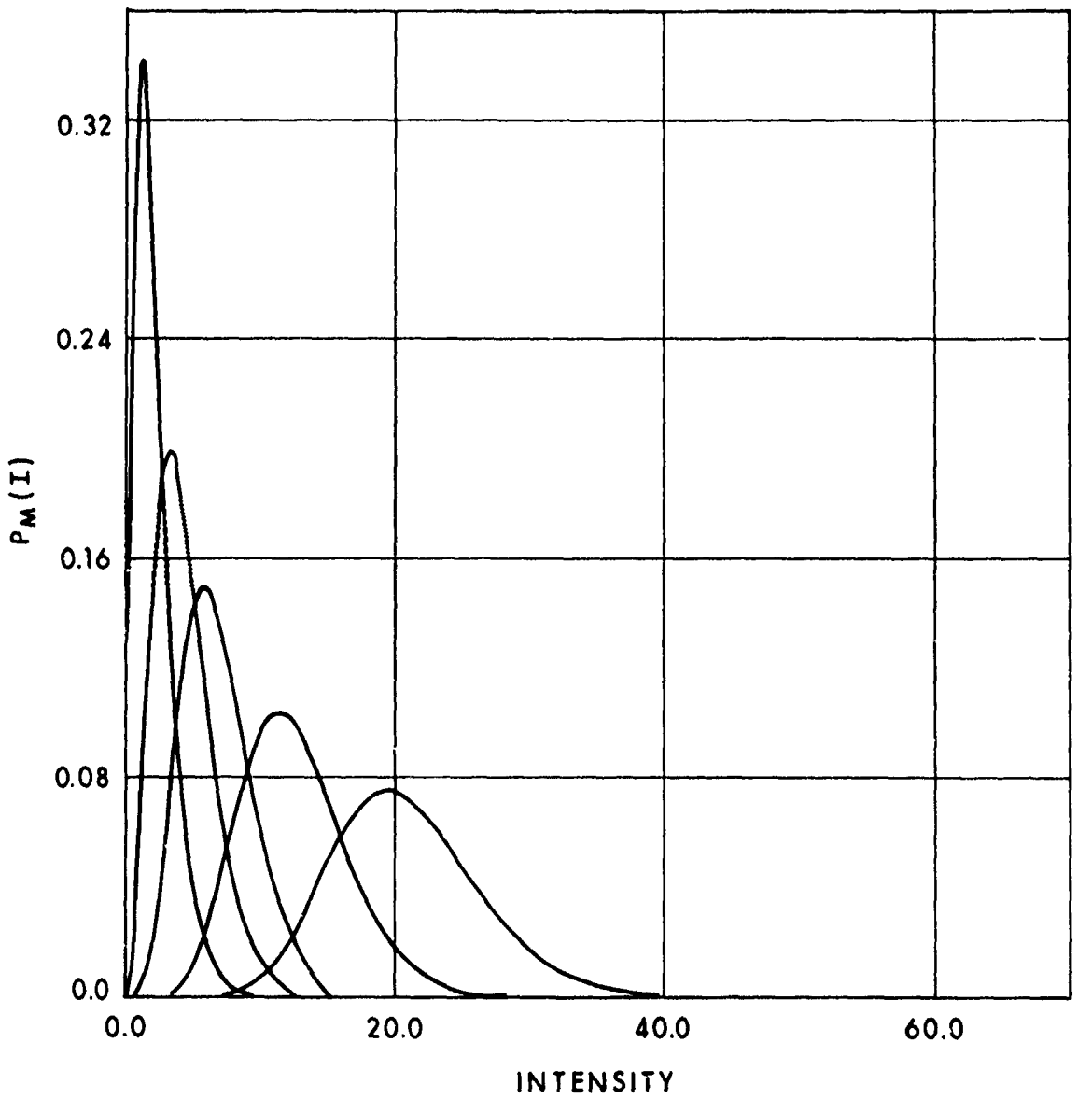

Fig. 7. The intensity probability distribution for M unequal variates with means satisfying $\lambda_i - \lambda_o + i \Delta I$, $i = 1, \ldots, M$. $\Delta I/\lambda_o = .05$

patterns which are obtained using energy detection. We now wish to obtain the probability distributions for systems which respond to the amplitude. We will first derive the density function for amplitude and then derive the density for M independe t amplitude distributions.

We wish to obtain the probability density for the variable $x = A/\sigma = I^{1/2}/\sigma$. Since

$$p(I) = \frac{1}{2\sigma^2} \exp(-I/2\sigma^2)$$

we have

$$p(x) = x \exp(-x^2/2)$$

and the moments of the normalized amplitude are given by

$$\overline{x^m} = \int x^{m+1} e^{-x^2/2} dx.$$

If we let $z = x^2/2$ we obtain

$$\overline{x^m} = 2^{m/2} \int_0^\infty z^{m/2} e^{-z} dz$$

$$= 2^{m/2} \Gamma\left(\frac{m+2}{2}\right)$$

with the first and second moments given by

$$\bar{x} = \sqrt{\frac{\pi}{2}}, \quad \bar{x}^2 = 2$$

which yields a square contrast factor of

$$C_A^2 = \frac{4}{\pi} - 1 = .27$$

which is much less than unity which was obtained for the intensity distribution. Note that the above amplitude distribution was normalized to $x = A/\sigma$ where 2σ is the second moment of A, i.e., this amplitude distribution has not been normalized to its mean, but rather, to its second moment.

The amplitude distribution may be normalized to its mean by the change in variables

$$x = \frac{\bar{A}}{\sigma} \; y \; = \sqrt{\frac{\pi}{2}} \; y$$

which yields

$$p(y) = \frac{\pi}{2} \; y \; \exp \; (-\frac{\pi}{4} \; y^2)$$

with moments given by

$$\overline{y^m} = \frac{2^m}{\pi^{m/2}} \; \Gamma \; (\frac{m+2}{2})$$

We now have

$$\bar{y} = 1, \; \langle A \rangle = \bar{A}$$

and

$$\overline{y^2} = \frac{4}{\pi}, \quad \langle A^2 \rangle = \frac{4}{\pi} \; \bar{A}^2$$

which yields the same square contrast factor of $C_A^2 = .27$.

We will now show the procedure for obtaining the amplitude probability distribution for M independent observations when there is no background term present. The technique is to find the characteristic function for one observation and then to raise the function to the Mth power. We then take the Fourier transform of the Mth power characteristic function.

If $\bar{A}$ denotes the mean value of the absolute value of the amplitude, then the normalized variable $y = A/\bar{A}$ yields the amplitude distribution.

$$p(y) = \frac{\pi}{2}\, y \, \exp\left(-\frac{\pi}{4} y^2\right)$$

where we have explicity eliminated the second moment 2σ which was used in the intensity distributions. The characteristic function corresponding to $p(y)$ is

$$C(w) = FT^{(+)}\,[p(y)]$$

$$= \frac{\pi}{2}\, FT^{(+)} \left[y\, e^{-\frac{\pi}{4} y^2} \right]$$

$$\simeq 4\pi i w \exp\{-4\pi w^2\}$$

where we have extended the values of y to $\pm\,\infty$. When y is large this does not yield a large error. And the Mth order characteristic function is given by

$$C^M(w) \simeq (4\pi i)^M\, w^M \exp\{-4\pi M w^2\}$$

The Mth order probability distribution is then given by

$$P_M(y) = FT^{(-)} \left[C^M(w)\right]$$

$$= 2^N \, FT^{(-)} \left[p^M \exp\left(+\frac{N}{\pi} p^2\right)\right]$$

$$y >> 1$$

where $p = 2\pi i w$. This Fourier transform is given in the transform tables of Campbell and Foster[3]. and is given by

$$P_M(y) = \left(\frac{\pi}{2}\right)^{\frac{M}{2}} \frac{1}{2\, M^{(M+1)/2}} \exp\left(\frac{\pi y^2}{4M}\right) H_M \left(\frac{\sqrt{\pi}}{\sqrt{2}} \frac{y}{\sqrt{M}}\right)$$

$$y >> 1$$

where H_M is the Mth order Hermite polynominal function and where we have extended the values of y to $\pm \infty$.

For the more realistic case of positive values for y we have

$$c(w) = FT^{(+)} \left[\frac{\pi}{2} \, y \exp\left[-\frac{\pi}{4} y^2\right]\right]$$

$$= \frac{\pi}{2} \int y \exp\left[-\frac{\pi}{4} y^2 + 2\pi i w y\right] dy$$

$$= \frac{2}{\pi} \left[1 - p \exp\left\{\frac{p^2}{\pi}\right\} \operatorname{erfc}\left\{\frac{p}{\pi}\right\}\right]$$

where $p = 2\pi iw$. The FT of the Mth power of $c(w)$ does not exist in closed form. Thus, for the case where we wish to know $p_M(y)$, for all $y > 0$, a closed expression is not obtained. Although $p_M(y)$ does not exist in closed form, we may obtain the first few moments of $p_M(y)$ from the moments of $p(y)$ as follows. It is shown in sec. 4.3 that

$$\bar{y}_M = M\bar{y}$$

$$\overline{y_M^2} = \overline{y^2} + M(M-1)\,\bar{y}^2$$

and since

$$\overline{y^M} = \frac{2^M}{\pi^{M/2}}\,\Gamma\left(\frac{M+2}{2}\right)$$

we obtain

$$\overline{y_M^2} = M\,\frac{4}{\pi} + M(M-1)$$

with a square contrast of

$$C_A^2 = \frac{\frac{4}{\pi} - 1}{M} \quad .$$

4.4 Specular Component Present

We have now seen that if the number of scatterers is very large and uniformly distributed the received intensity follows a Rayleigh distribution in amplitude or a negative exponential distribution in intensity. However,

these statistical distributions are not obtained if the scatterers are nonuniformly spread over the target area, i.e., if the target reflection is a function target position or if a specular component is present.

Let A_R represent the part of the amplitude which is not normally distributed and is a result of the changing target reflectivity. Then the amplitude may be written as

$$A = \left[(A_1 + A_R)^2 + A_2^{\,2} \right]^{1/2}$$

and we then inquire as to the form of the probability distribution of this new variable.

The new probability density has the form of a Rician distribution and is given by

$$P_R(A) = \frac{A}{\sigma^2} \exp \left[- 1/2 \, (A^2 + A_R^{\,2}) / \sigma^2 \right] x$$

$$I_o \, (AA_R/\sigma^2)$$

where $2\sigma^2$ is the mean square amplitude of the sum of the oscillations and where $I_o \, (AA_R/\sigma^2)$ is a modified Bessel function of order zero. This distribution is obtained as follows. The joint gaussian distribution in the presence of the real signal is

$$d^2P(A_1,A_2) = \frac{dA_1 dA_2}{2\pi\sigma^2} \exp\left\{-\left[(A_1-A_R\cos\beta)^2 + (A_2-A_R\sin\beta)^2\right]\Big/2\sigma^2\right\}$$

$$d^2P(A_1,A_2) = \frac{dA_1 dA_2}{2\pi\sigma^2} \exp\left\{-\left[A_1^2 + A_2^2 - 2A_1A_R\cos\beta - 2A_2A_R\sin\beta + A_R^2\right]\Big/2\sigma^2\right\}$$

and since

$$A_1 = A\cos\alpha,\ A_2 = A\sin\alpha$$

we change to polar coordinates

$$d^2P(A,\alpha) = \frac{AdAd\alpha}{2\pi\sigma^2} \exp\left\{-\left[A^2 - 2AA_R\cos(\alpha-\beta) + A_R^2\right]\Big/2\sigma^2\right\}$$

and the density dP(A) is obtained from

$$dP(A) = \int d\alpha\ dP\ (A,\alpha)$$

$$= \frac{AdA}{\sigma^2} \exp\left\{-\frac{(A^2 + A_R^2)}{2\sigma^2}\right\} I_0\ (AA_R/\sigma^2)$$

where

$$I_0\ (AA_R/\sigma^2) = \frac{1}{2\pi}\int d\alpha \quad \exp\left\{\frac{AA_R}{\sigma^2}\right\}\cos\alpha$$

Note that the original RMS noise was given by σ and we thus write

$$s = A_R/\sigma$$

as the reflected amplitude signal to noise ratio. Let the amplitude be measured in units of σ and define the statistical parameter

$$x \equiv A/\sigma$$

and the density function becomes[4-5]

$$p(x,s) = x \exp \left[- (x^2 + s^2)/2 \right] I_0(sx)$$

This density function is the Rician distribution and is plotted in Figure 8 for several amplitude signal to noise ratios.

The first, second, and fourth moments are given by Rice[6] to be

$$\bar{x} = 1/2 \ (2\pi)^{1/2} \exp \ (-s^2/4) \left[(1 + \frac{1}{2} s^2) \ I_0 \ (s^2/4) + s^2 \ I_1 \ (s^2/4) \right]$$

$$\overline{x^2} = (2 + s^2)$$

$$\overline{x^4} = (8 + 8s^2 + s^4).$$

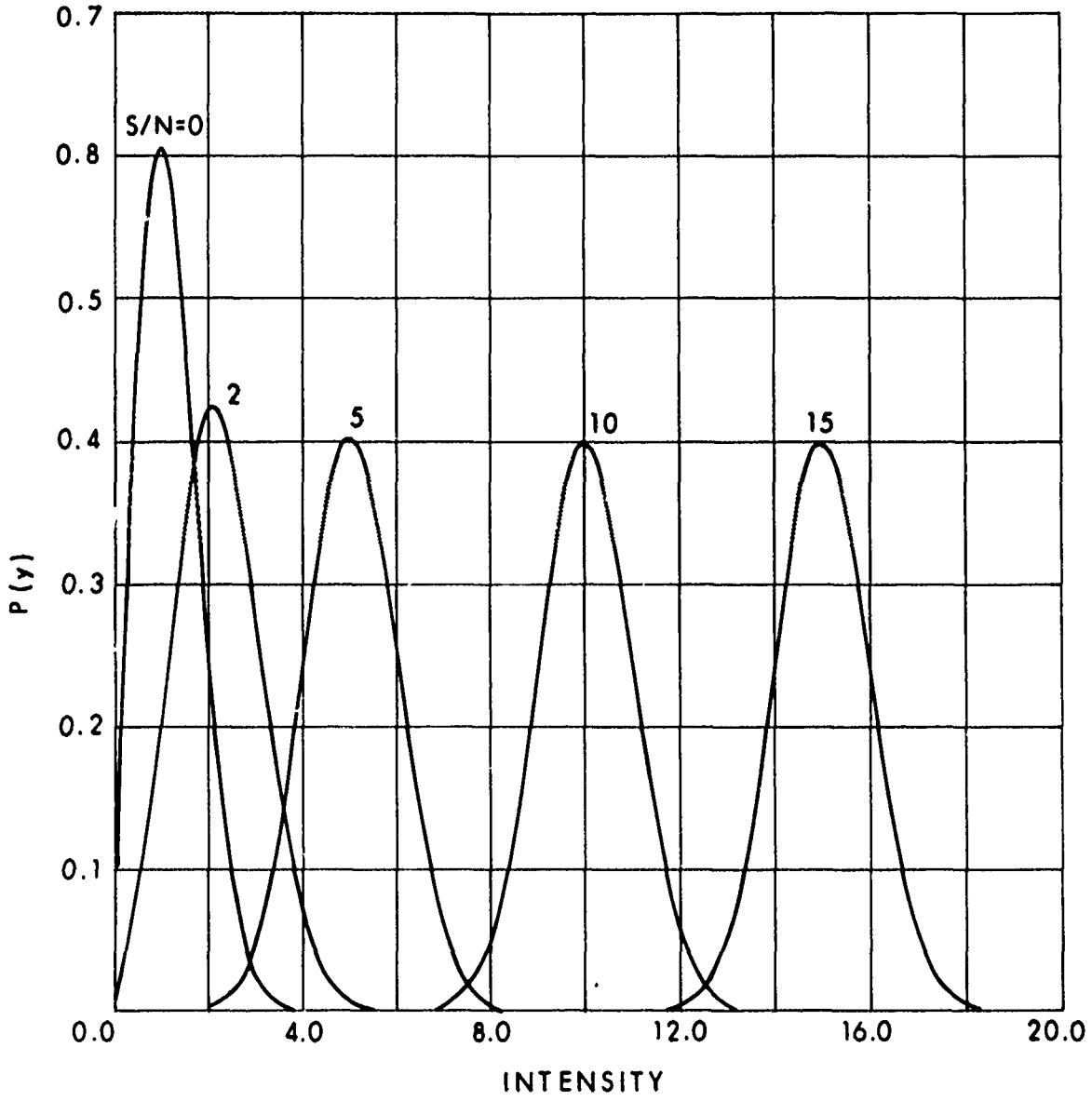

Fig. 8. Probability density for the Rician distribution for several values of the amplitude envelope signal to noise ratio.

The probability distribution in intensity is given by

$$P(I) = \frac{1}{2\sigma^2} \exp \left[-\frac{1}{2\sigma^2} (I + I_R) \right] I_o \left[\frac{I^{1/2} I_R^{1/2}}{\sigma^2} \right]$$

where I_R is the specular component in intensity. If $r = I_R/\sigma^2$ is identified as the intensity S/N, and we make all intensity measurements with respect to σ^2 we may define $y = I/\sigma^2$ and obtain

$$p(y) = 1/2 \exp \left[- 1/2 (Y + r) \right] I_o (y^{1/2} r^{1/2})$$

which is the normalized intensity distribution in the presence of a signal. Note that

$$\text{Lim } p(y) = \frac{1}{2\sigma^2} \exp (-I/2\sigma^2)$$

which is the negative expontial distribution obtained in section 4.1 p(y) is shown in Figure 9 for r = .01, 1, 4, 9, and 16. Now, since

$$\overline{y} = \overline{x^2}$$

$$\overline{y^2} = \overline{x^4}$$

and

$$r = s$$

TT-9 (9)

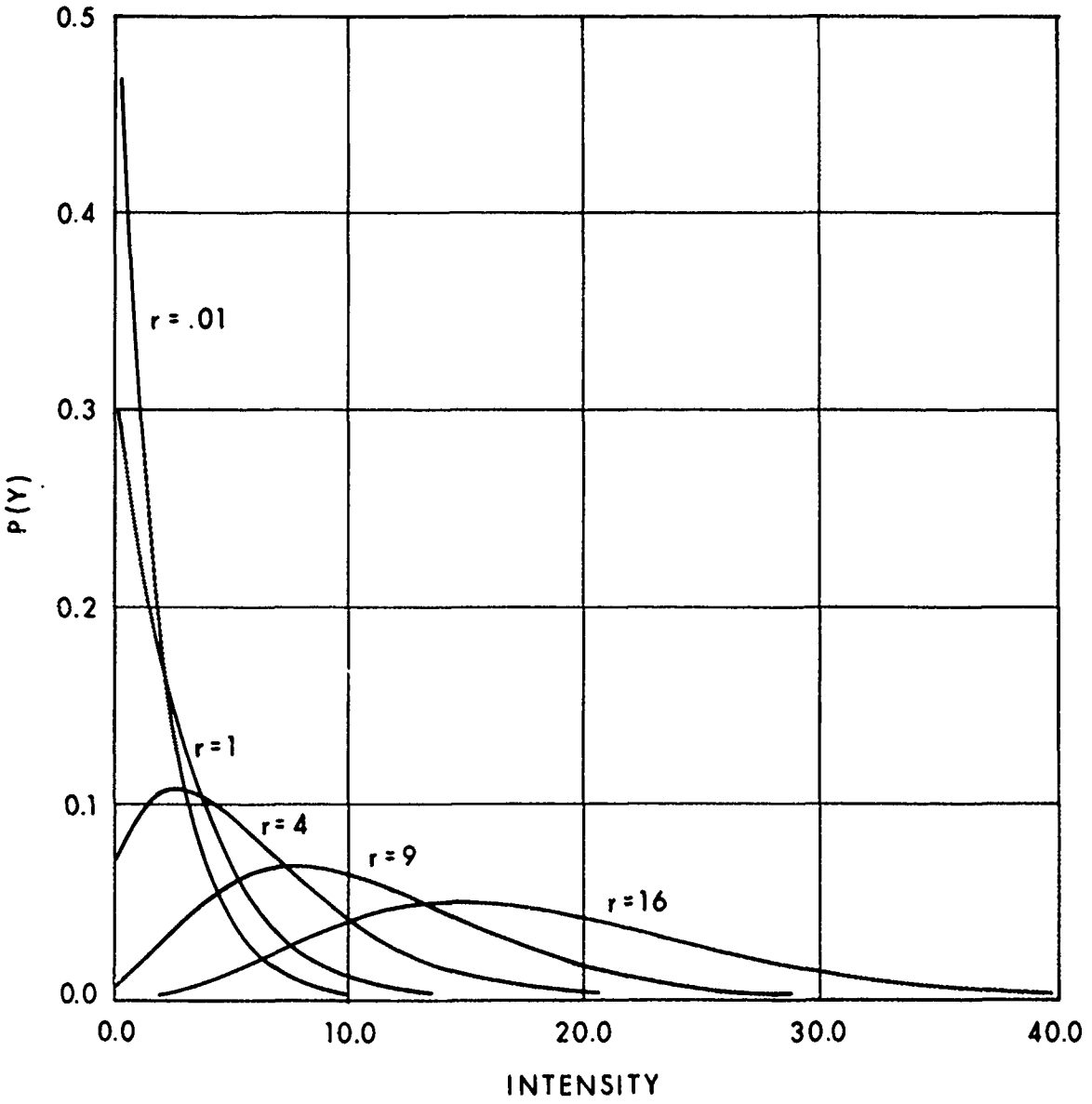

Fig. 9. The intensity distribution for several values of the intensity signal to noise ratio.

the first and second intensity moments are given by

$$\bar{y} = 2 + r$$

$$\overline{y^2} = 8 + 8r + r^2$$

with the variance

$$\overline{y^2} - \overline{y}^2 = 4\,(1 + r)$$

with a square contrast

$$C_I^{\,2}(r) = \frac{4(1 + r)}{(2 + r)^2}$$

which is shown in Figure 10.

4.5 The Addition of Independent Distribution in the Presence of Background

Let us now consider the case where we wish to combine M independent noise patterns each described by $p_i(y_i r_i)$

$$y_i = \frac{1}{\sigma_i}, \quad i = 1, \ldots, M$$

$$r_i = I_i / \sigma_i$$

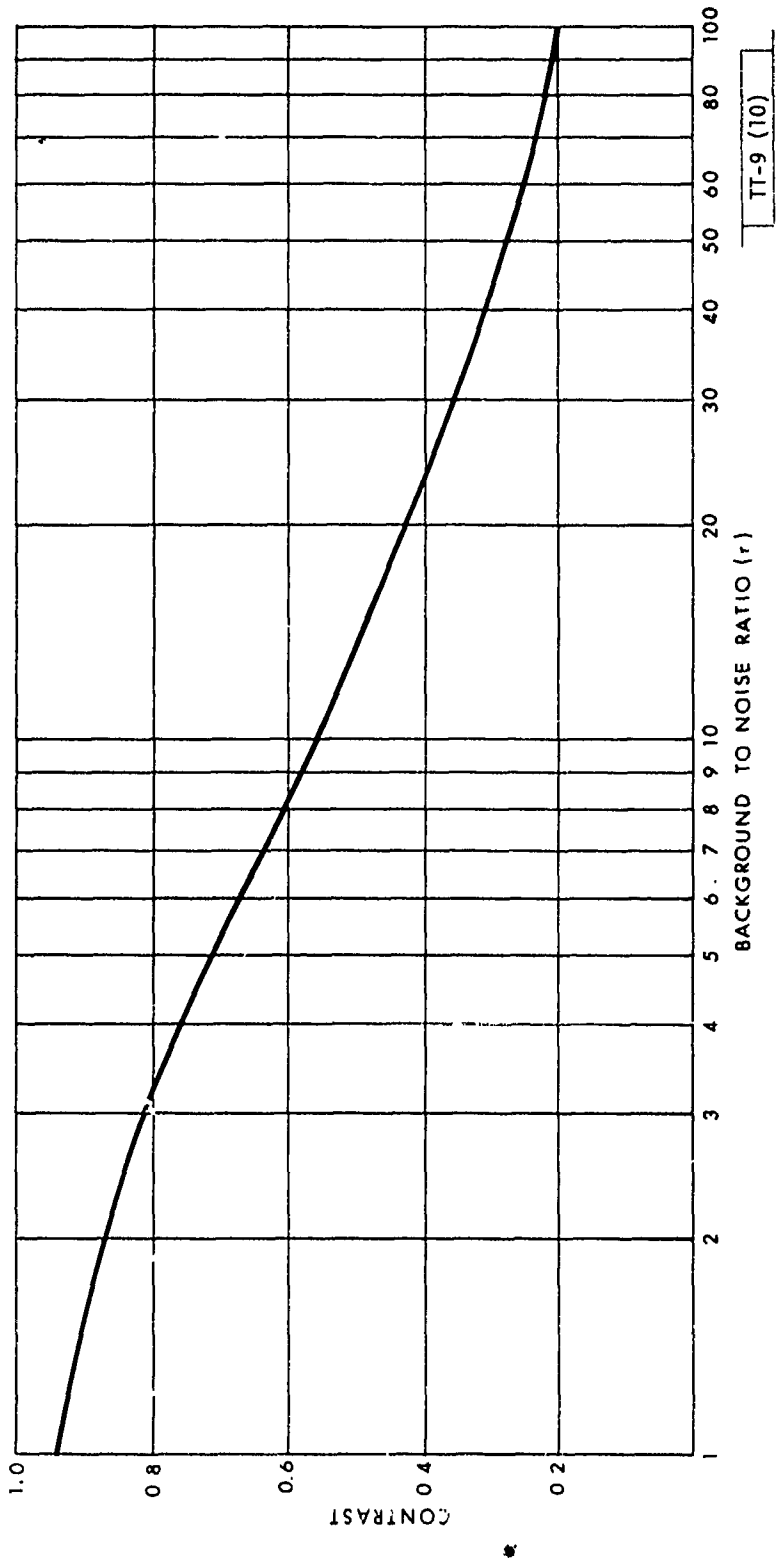

Fig. 10. The square amplitude envelope contrast as a function of background signal to noise ratio.

The new probability distribution $p_M(y)$ is given by

$$P_M(y) = FT^{-1} \left[C_M(\omega)\right]$$

where $C_M(\omega)$ is the characteristic function

$$C_M = \prod_{i=1}^{M} c_i(\omega)$$

$$c_i(\omega) = FT \quad p_i(y_i, r_i)$$

However, the Fourier transform of $p_i(y_i, r_i)$ does not exist in closed form and the distribution is difficult to express in a finite number of terms.

However, if the M^{th} moment $b_{m,j}$ of $p_i(y_i, r_i)$ is known we can obtain the moments a_m^M from the characteristic function since the M^{th} moment of $p_M(y)$ is given by

$$a_m^M = (-1)^m \frac{d^m}{d\omega^m} C_M(\omega) \Big|_{\omega=0}$$

$$= (-1)^m \frac{d^m}{d\omega^m} \prod_{j=1}^{M} c_j(\omega) \Big|_{\omega=0}$$

where

$$b_{m,j} \equiv (-1)^m \frac{d^m}{d\omega^m} c_j(\omega) \Bigg|_{\omega=0}$$

We consider the case where the M distributions $p_i(y_i, r_i)$ are equal. Then

$$C_M(\omega) = c^M(\omega)$$

and

$$a_m^M = (-1)^m \frac{d^m}{d\omega^m} c^M(\omega) \Bigg|_{\omega=0}$$

The first and second moments are

$$a_1^M = Mb_1$$

and

$$a_2^M = Mb_2 + M(M-1)b_1^2$$

and the moments in the intensity are given by

$$\overline{y_M} = M(2 + r)$$

$$\overline{y_M^2} = M(8 + 8r + r^2) + M(M-1)(2+r)$$

with the variance

$$\overline{y_M^2} - \overline{y}_M^2 = 4M\,(1+r)$$

and the mean square contrast is

$$C^2(r,M) = \frac{4(1+r)}{M(2+r)^2}$$

The contrast improves with $M^{-1/2}$ as expected.

4.6 Correlated Intensity Distributions

So far we have treated diffuse scintillation images as having independent statistics and we now wish to investigate the more complicated problem of patterns with a non-zero correlation. We will treat the addition of two correlated speckle patterns in the absence of a signal.

Let $A = A_1 + iA_2$ and $B = B_1 + iB_2$ correspond to fields from the two patterns. We treat A_1, A_2, B_1, and B_2 as normally distributed variates with equal weight. The fourth order joint probability density is given by

$$P(A_1, A_2, B_1, B_2, \rho) = \frac{1}{(2\pi\sigma^2)^2\,(1-\rho^2)^2}$$

$$\exp\left\{-\frac{1}{2\sigma^2(1-\rho^2)}\left[A_1^2 + A_2^2 + B_1^2 + B_2^2 - 2\rho(A_1 B_1 + A_2 B_2)\right]\right\}$$

where ρ is the correlation coefficient which varies from one to zero[7]

We change variables to the polar form of

$$A_1 = A\cos\gamma, \quad A_2 = A\sin\gamma$$

$$B_1 = B\cos\delta, \quad B_2 = B\sin\delta$$

which gives

$$dA_1 dA_2 dB_1 dB_2 = |J|^{-1} \, dA dB d\gamma d\delta$$

$$= AB dA dB d\gamma d\delta$$

where the Jacobian is given by $(AB)^{-1}$.

The new joint density is given by

$$p(A,\gamma;\, B,\delta) = \frac{AB}{(2\pi\sigma^2)^2 \, (1-\rho^2)} \exp\left[\frac{-1}{2\sigma^2 \, (1-\rho^2)} \, (A^2 + B^2) - 2\rho\cos(\gamma-\delta)\right]$$

The joint distribution $p(A,B)$ is obtained by integrating over γ and δ from 0 to 2π. Note that only the phase difference $\gamma-\delta$ appears in $p(A,\gamma;\, B,\delta)$. Since the reference phase is arbitrary we set $\gamma = 0$ and obtain

$$p(A,B) = \iint_0^{2\pi} d\gamma dB p(A,\gamma;\, B,\delta)$$

$$= \frac{AB}{\sigma^4(1-\rho^2)} \exp\left\{-\frac{A^2 + B^2}{2\sigma^2(1-\rho^2)}\right\} x$$

$$I_o\left(\frac{\rho AB}{\sigma^2(1-\rho^2)}\right)$$

where, as in section 4.3, $I_0(x)$ is the zero order Bessel function of the with an imaginary argument,

$$I_0(x) = J_0(ix)$$

$$= \frac{1}{2\pi} \int_0^{2\pi} d\phi e^{x\cos\phi}$$

The density in intensity variables

$$I_1 = A^2, \quad I_2 = B^2$$

is

$$p(I_1, I_2) = \frac{1}{\sigma^4(1 - \rho^2)} \exp\left\{-\frac{I_1 + I_2}{2\sigma^2(1-\rho)}\right\} x$$

$$I_0\left(\frac{\rho I_1^{1/2} I_2^{1/2}}{\sigma^2(1-\rho^2)}\right)$$

and the density in terms of the variable[8]

$$I = I_1 + I_2$$

$$P(I) = \int_{-\infty}^{+\infty} p(I_1, I-I_2)\, dI_1$$

$$= \exp\left\{ - \frac{1}{2\sigma^2(1-\rho)} \right\} F(I,\sigma;\rho)$$

where $F(I,\sigma;\rho)$ is given by

$$F(I,\sigma;\rho) = \int_0^I I_o \left(\frac{\rho I_1^{1/2}(I-I_1)^{1/2}}{2\sigma^2 (1-\rho)} \right) dI_1$$

The function $F(I,\sigma;\rho)$ is not available in closed form and must be obtained numerically.

5. DIFFUSE TARGET SCINTILLATION REDUCTION

We will describe four methods of obtaining statistically independent observations of diffuse sources. These methods may be summarized as:

1. Spatial Averaging
   a. Multiple observations
   b. Multiple receiver apertures
   c. Multiple transmitter apertures
2. Angular Averaging
   a. IFOV overdesign
   b. Multiple IFOV elements
3. Polarization Averaging
4. Frequency Averaging

In this discussion that follows we will assume the system uses heterodyne detection and that the receiver IFOV matches the transmitter beam divergence. Since a heterodyne receiver is diffraction limited the receiver aperture will be fixed once the transmitter divergence has been chosen from a consideration of range and required spot size. If direct detection was employed one could employ a larger receiving aperture and thereby obtain a reduction in speckle directly through aperture averaging. However, for coherent systems this freedom does not exist and one must employ these techniques listed.

5.1 Spatial Averaging

Multiple Observations

The technique of multiple spatial observations is based on the fact that if the laser radar is translated a coherence length and a new image is observed then this image will have independent speckle statistics.[9] The images may then be combined to reduce the scintillation effects. If an aircraft is moving over a scene with a speed V, then the time required to make a second observation is given by $\Delta t = L_C/V$. For the special case where $L_C \cong D_T$, Δt is the time required for the aircraft to move the distance equal to the transmitter diameter. The worst case occurs for slow moving aircraft, 3,000 cm/sec, say, and for D_T = 10 cm, we obtain $\Delta t = 3 \times 10^{-3}$ sec, which is an order less than a typical line scanner frame time. In this case, multiple frames could be combined and the major problems would be roll and vibrational stability to obtain accurate image registration. For

example, if ten frames were to be combined, we would require an angular stability of one IFOV element over the time it took for the registration of ten frames. To simulate these independent observations in the laboratory one can rotate the target with respect to the laser axis.

Another problem to be addressed is the image storage and eventual addition. Image storage tubes could be employed and the storage and additions using CCD's and CID's hold particular promise.

It should also be pointed out that if many observations are required an increase in scanner speed may not always be practical. For example, with imaging systems that also require high doppler resolution, there is a minimum detector dwell time (and, therefore, an upper limit on scan speed) given by

$$t_d \gtrsim \frac{\lambda}{2\delta v}$$

where δv is the required doppler resolution.

Multiple Transmitter and Receiver Apertures

A second technique using spatial averaging is to employ a multiplicity of receiver and/or transmitter aperatures which are separated by a correlation distance L_C. In the ideal case where the correlation distance is a transmitter diameter we would have to maintain separations of the order of 10 cm for 10.6μm systems. This type of separation is not difficult to obtain and should not cause major design problems. However, multiple transmitter and receiver optics must be re-aligned every time the altitude is changed. This re-alignment is necessary so as to maintain

the receiver IFOV directly on the laser illuminated target. Techniques for a continual alignment with altitude have not been developed and a feasibility investigation should determine how the S/N and angular resolution degrade in systems with automatic alignment.

5.2 Angular Averaging

IFOV Overdesign

A straightforward method for reducing speckle in a coherent laser line scanner is to design the system for more angular resolution than is required for a particular application. A highly speckled pattern will be obtained but since there is more angular resolution available, one may average adjacent high resolution elements and thereby obtain an angular average with a corresponding decrease in speckle. If photographs are required the procedure is simple. Place the high resolution speckled photograph in the out of focus region of a camera and take a second, slightly out of focus, photograph. The new photograph will have less speckle and less angular resolution since it was obtained with the camera slightly out of focus. Of course, there is no practical reason why one would want to produce the second photograph because it does not contain any more information than exists in the first photograph. However, for systems that operate in real time and are to obtain automatic target identification such a reduction technique is necessary and must be accomplished through electronic storage and addition.

The price one pays for this type of averaging is that for constant frame rates the IFOV dwell time is decreased with a corresponding increase in system bandwidth. Although one increases the noise due to the increase in the post detection bandwidth one gains signal when the adjacent high resolution elements are combined with the result that the final signal to noise is the same as what would have been obtained with an instrument designed for the lower angular resolution. Note that in order to obtain a smaller spot size one must decrease the transmitter divergence. Similarly one must use a smaller receiver IFOV which, for diffraction limited coherent systems, implies a larger receiver aperture.

A diversity of at least two can be obtained for imagers that use a continuous raster scan across a diffuse target. To see this it is only necessary to compute the number of independent illuminated spots that are recorded in every dwell time.

Let the illuminated spot diameter be given by D_{Targ}. Then the number of independent speckle patterns obtained in one dwell time is given by

$$n_s = 2\frac{D_S}{D_{Targ}}$$

where D_S is the distance scanned by the illumination spot in a dwell time t_D. D_S is given by

$$D_S = R \overset{\circ}{\Theta} t_D = R \Theta_R$$

where $\dot{\Theta}$ is the scan rate and Θ_R is the receiver IFOV. For a laser transmitter, the target spot diameter is

$$D_{Targ} = R\,\Theta_T$$

where Θ_T is the transmitter divergence and

$$n_S = 2\,\frac{\Theta_R}{\Theta_T}$$

and for a diffraction limited transmitter and receiver

$$n_S = 2\,\frac{D_T}{D_R}$$

For a heterodyne transmitter/receiver sharing the same aperture we obtain $n_S = 2$.

Multiple IFOV Elements

In the previous section, we found that by using IFOV overdesign and combining adjacent high resolution elements the speckled appearance of a photograph could be improved but its photon signal would remain the same Now consider a vertical fan beam which sweeps the scene horizontally. Let this vertically formed spot be followed by a receiver with n_y vertically placed detectors. With this design there are n_y independent IFOV elements associated with just one fan shaped laser beam. Each IFOV element sees a different part of the laser illuminated spot. If each partially illuminated spot can be regarded as an independent source with statistics uncorrelated to the other adjacent spots then each IFOV element will obtain an independent set of fluctuations. As the aircraft mounted sensor moves forward in

the direction of the vertical beam each IFOV ground element may be observed by adjacent detectors and, with appropriate storage and time delay, averaging may be obtained without a higher information bandwidth.

The problems associated with designing and operating a coherent focal plane array are mostly concerned with how one matches one local oscillator signal to many detectors. Quadrant and five element linear arrays have been employed in coherent sensors and a feasibility investigation should identify what problems would be associated with a nine element (three by three) array. A ten element linear array with a matched fan also deserves careful consideration.

In applications where a multi-element focal plane is required it is desirable to place the detectors as close as possible. However, optical cross talk should be minimized to 30 or 40 dB which will demand that the detectors be spaced approximatley 10% of the diffraction limited detector size. If the spacing technique does not yield the required cross talk attenuation, one will have to consider an optically shielded plane array.

The coherence distance has been shown to be given by $L_C \cong R\lambda/L_{Targ}$. This is the distance at the aperture plane over which there exists a spatial amplitude correlation. Now consider a direct detection imager with transmitter and receiver aperture given by D_T and D_R, respectively. If the transmitter is diffraction limited, the target diameter is given by

$$L_{Targ} \cong R \frac{\lambda}{D_T}$$

and the coherence distance is given by

$$L_{Targ} \cong D_T$$

and the number of independent coherence regions in the receiving aperture area is given by

$$N = \frac{A_R}{\frac{\pi}{4} L_C^2}$$

$$\cong \left(\frac{D_R}{D_T}\right)^2$$

N is therefore the number of independent speckle patterns which will be incoherently combined at the direct detection focal plane. Thus, if the receiver aperture is made larger than the transmitter aperture, a spatial averaging will be obtained in a direct detection receiver. However, for heterodyne receivers employing a single detector, this type of aperture averaging is not possible.

The reason why a single detector heterodyne receiver cannot be employed in an aperture averaging system is due to the fact that heterodyne detection employs amplitude reception. The size of the effective aperture in a heterodyne receiver is only as large as the region of high amplitude correlation across the aperture plane. Thus, if the receiver aperture is made larger than the coherence distance L_C the receiver will have a signal strength proportional to L_C^2 and not to the physical size of the receiver.

Now this limitation of a heterodyne receiver may be circumvented by employing an aperture diameter, D_H, which is larger than the coherence

distance, L_C, in conjunction with a focal plane array of detectors. Each detector will be sized to the diffraction limit, i.e.,

$$IFOV \cong \frac{\lambda}{D_H}$$

and the combined square array field of view will be matched to the coherence region, i.e.,

$$\Theta_{array} \cong \frac{\lambda}{L_C}$$

$$= L_{Targ}/R$$

which is just the subtense of the illuminated target.

Each individual detector in the focal plane array will observe a small fraction of the illuminated spot as is shown in Figure 11. The target observation diameter is

$$L'_{Targ} = IFOV.R$$

$$= \frac{\lambda}{D_H} R$$

where D_H is the heterodyne aperture which is larger than the transmitter aperture diameter D_T.

The observation spot will be the source of a new coherence patch of diameter

$$L_C = \frac{\lambda}{L'_{Targ}} R$$

$$= D_H$$

but the plane of this coherence patch will be tilted with respect to the aperture plane by an angle of the order r_i/R where r_i is the distance from the center of the target illumination area to the i^{th} observation circle corresponding to the i^{th} element in the focal plane array. r_i is shown in Figure 11.

Since all the target subregions have a constant phase relationship to one another, we must incoherently add the output from each detector to obtain a speckle reduction. This would be equivalent to having each subregion illuminated by lasers with no spatial correlation. The amount of speckle reduction is then just the number of detectors in the focal plane array which is given by

$$N_A = \left(\frac{\Theta_{array}}{IFOV}\right)^2$$

$$= \left(\frac{\lambda/D_T}{\lambda/D_H}\right)^2 = \left(\frac{D_H}{D_T}\right)^2$$

which is the same number of independent speckle patterns obtained in the direct detection system. Note that we have assumed an extremely close spacing between each element of the focal plane array. The fact that we have obtained the same aperture averaging as the direct detection receiver should not be surprising if one recognizes that, by the incoherent addition of N_A detectors in a square array (which has the same total angular subtense as the direct detection system), we have, in effect, produced a direct detection receiver with the photon sensitivity of a heterodyne system.

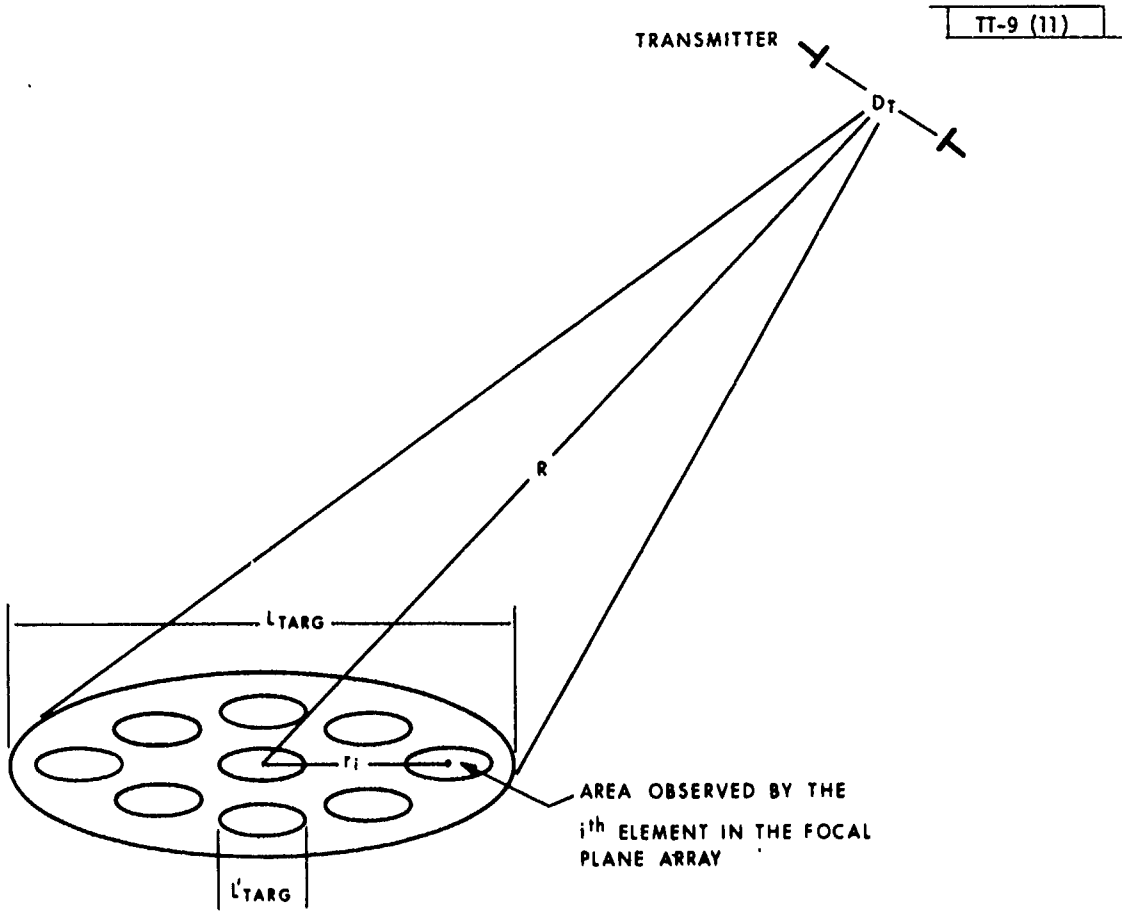

Fig. 11. The focal plane array observation of an illuminated area of diameter L_{Targ}. Each element in the array observes a sub-element of diameter L'_{Targ}.

5.3 Polarization Averaging

The laser target illumination is plane polarized whereas the reflected beam is partially depolarized. The partial target depolarization is dependent on the surface characteristics and very little information exists on target polarization properties. Two independent polarized fields will be obtained in the far field and these fields will have independent diffuse target scintillation statistics and may thus be combined to reduce the speckle.[9] The amount of speckle reduction depends on the percentage of target depolarization. It is clear that if a target converts 50% of its reflected photons into each independent polarization component then a diversity of two may be obtained and the speckle noise may be reduced by .707.

To obtain polarization averaging two detector focal planes must be employed. Each focal plane must utilize local oscillators with perpendicular polarization components. This appears to be a considerable hardware effort to obtain a maximum diversity of two. However, there are further advantages to using a dual-polarized receiver. The signal to noise of such a system is improved by a maximum of two since, in a single-polarized receiver, all depolarized photons are not mixed with the local oscillator. A further advantage is obtained when one recognizes that target identification and MTI detection probabilities can be enhanced since man-made targets will often have different polarization characteristics than natural terrain background. Thus, given a mission which demands a probability of detection

with a given false alarm level, the required signal to noise can thereby be reduced.

It should be pointed out that if one wishes to investigate polarization effects on coherent imagers it is not necessary to employ a dual detection system if one employs a system with separate transmitter and receiver. With such a system, one can obtain laboratory data by first obtaining an image for a fixed polarization and then obtain a new image with the relative receiver/transmission polarization rotated by 90^{o}. The two images will then have independent scintillation statistics and will yield the required information on target depolarization. Rather than build a system with a dual polarization capability, it is first necessary to experimentally determine the degree of depolarization for various targets.

We wish to obtain the probability of density for a partially polarized diffuse signal which is obtained by a detection system which responds independently to both degrees of polarization. Let the degree of polarization by given by P and the mean intensity in each beam be given by

$$I_1 = 1/2\ (1 + P)\ \bar{I}$$

$$I_2 = 1/2\ (1 - P)\ \bar{I}.$$

Since the polarization measurements are independent we have for the characteristic function

$$C(z) = \left[1 - \frac{i}{2}\ (1 + P)\bar{I}z\right]^{-1} \left[1 - \frac{i}{2}\ (1 - P)\bar{I}z\right]^{-1}.$$

The probability density function is obtained from the Fourier transform of C(z) and we have

$$P(I) = \frac{1}{2\pi} \int_{-\infty}^{+\infty} \frac{e^{z\pi i z I} dz}{\left[1 - \frac{i}{2}(1+P)\bar{I}z\right]\left[1 - \frac{i}{2}(1-P)\bar{I}z\right]}$$

which can be solved using Cauchey's integral theorem giving

$$P(I) = \frac{1}{P\bar{I}} \left\{ \exp\left(\frac{-2I}{(1+P)\bar{I}}\right) - \exp\left(\frac{-2I}{(1-P)\bar{I}}\right) \right\}$$

Figure 12 shows P(I) for $\bar{I} = 1$ and for the polarization values of P = 1.0, P = .75, P = .50.

5.4 Frequency Averaging

In the section on the wavelength dependence of the diffuse scintillation patterns it was shown that, due to the temporal coherence of the transmitter signal, the pattern would be uncorrelated provided that the effective spectral width of the source satisfied

$$\Delta\lambda > \frac{\lambda^2}{2\ell_o}$$

where ℓ_o is the mean depth of the diffuse target which is shown in Figure 3. ℓ_o was also shown to be the effective size of a resolution element when the angle of incidence is oblique to the target normal (see Figure 4).[9]

Now for an aircraft radar with an angle of incidence 45^o the effective decorrelation length L_C is given by cos $(\pi/4)$ L_T, where L_T is the

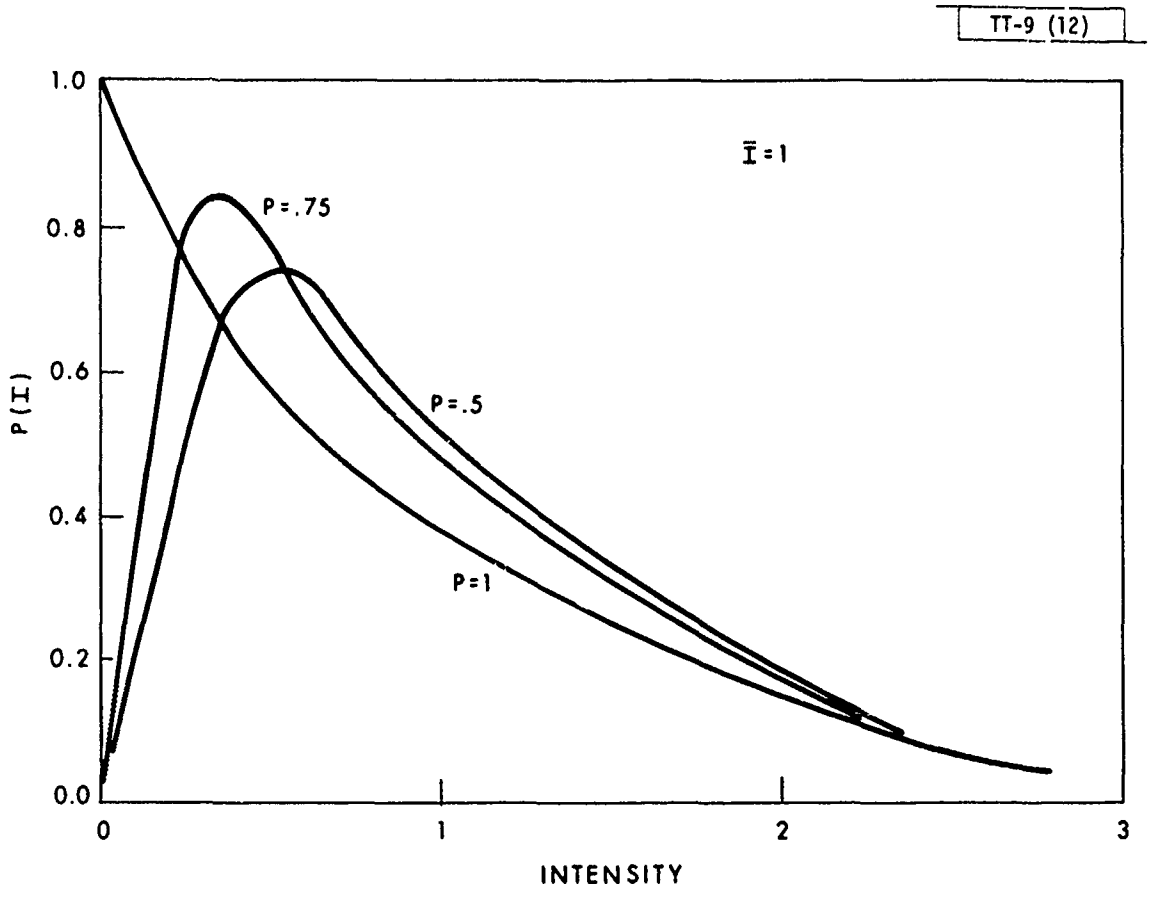

Fig. 12. Probability density for a dual polarization heterodyne receiver.

normal target size and the required frequency separation is given by

$$\Delta\sigma = \frac{1}{2 L_T}$$

which is 5×10^{-3} cm^{-1} for a target size of one meter. This corresponds to a frequency difference of 150 MHz. Thus, if the laser spectrum has a width of at least 150 MHz and frequency bins are employed in the receiver, we may obtain independent speckle patterns from each bin separated by this frequency difference.

Consider the situation where the transmitter consists of M narrow spectral lines of equal intensity but separated from one another at frequency intervals $\Delta\nu$. We require a detector which will be able to discriminate between the M different frequencies. This could be accomplished by using the heterodyne beat frequency of a local oscillator whose center frequency was within the power spectrum of the laser transmitter.

The output from each frequency bin would then be incoherently added to obtain an improvement of M in the speckle signal to noise, where M is the number of spectral lines which are effectively employed. It should be pointed out that this system only becomes practical where very large bandwidths can be tolerated in a design or where the oblique target spot size is much larger than one meter. For example, in a ground mapping mission where the oblique target size is 10 meters then the required bandwidth separation would only be 15 MHz and considerable improvements in speckle contrast could be obtained with a broad band laser source and a large number of frequency bins.

Note also that frequency averaging requires the application of a local oscillator which is independent of the transmitter. In some applications this is an added complexity which requires additional weight and optical alignment requirements.

6. Diffuse Target Scintillation Measurements

A summary of Rayleigh and Rician statistics has been given and we wish to emphasize here that the expected statistics must be verified experimentally by measuring the higher moments of the fluctuation. It should also be demonstrated that the correlation distance satisfies $L_C \cong R(\lambda/L_{Targ})$ and that the moments of the fluctuations are independent of L_{Targ} provided that there exist many independent scatters in the target area.

The moments of the fluctuations should be measured for a variety of sources to see if there is a difference in the far field amplitude pattern for different surfaces. The correlation distances should also be measured for various diffuse sources and the inverse dependence of the correlation distance on the target spot size should be verified, that is, $L_C = R(\lambda/L_{Targ})$.

For each diffuse source we will also need to know the ratio of diffuse to specular reflectivity and if the reflectivity varies across the surface.[10] From this preliminary investigation of diffuse materials a few must be selected to construct the appropriate bar charts which we will now discuss.

The quantitative evaluation of coherent images will be obtained from a diffuse bar chart whose surface requirements are to be determined

experimentally. The type of measurements that must be made with the diffuse bar chart area fall into the categories of the system NE$\Delta\rho$ and image resolution.

The coherent system noise equivalent reflectivity degradation must be measured. This may be accomplished by using bar chart backgrounds which are diffuse and differ in average reflectivity. The bar chart must be separated into two parts: target and variable reflectivity background. As the reflectivities of the bar targets and background are brought closer together the percentage of speckle noise will be obtained directly from the NE$\Delta\rho$. Improvements in the NE$\Delta\rho$ should be observed in the speckle reduction experiments which will be discussed in a later section.

The coherent sensor angular resolution degrades with increasing diffuse target scintillation. While the NE$\Delta\rho$ experiments are being performed the angular resolution of the system may be obtained from the diffuse bar chart which is constructed of diffuse bars of varying spatial separation. The final result of the experiment will be the graphical presentation of angular resolutions dependence on NE$\Delta\rho$. Once this type of relation is obtained for different diffuse sources, one may then determine the required quantitative speckle reduction for a system to yield a given angular resolution and NE$\Delta\rho$.

An investigation should be conducted to determine if the diffuse surface fluctuations distort the edges of man-made objects. For example, it is not known if a diffuse background will create granular effects along

a straight edge. This edge distortion appears qualitatively in coherent images but its origin is poorly understood. This effect can be seen when imaging a plane on a runway. Often the edge of the winds have a rough texture and it is not known if this noise is due to edge diffraction, glints, or diffuse fluctuations. It would be a straightforward procedure to place straight edged objects above a diffuse background and determine the degree of the diffuse scintillation contribution.

After the contrast and angular resolution measurements have been performed, it is then necessary to demonstrate that the speckle may be reduced by a variety of techniques. In particular, it should be demonstrated that by moving the receiver a correlation distance and obtaining a new image pattern one obtains a reduction in speckle contrast with an improvement in angular resolution. The improvement in contrast and angular resolution should be graphed as a function of the number of observations. If the contrast does not improve as the square root of the observation number, then the observations are partially correlated and the receiver correlation distance must be increased and the experiment should be repeated. In order to perform the measurements which have been discussed it is necessary to employ a laser line scanner with characteristics suitable for a scintillation reduction investigation.

The instantaneous field of view for the coherent sensor should be between .05 mrad and .5 mrad. The .5 mrad IFOV will be subject to less atmospheric scintillations in experiments where the transmit/receiver path

is greater than a few kilometers. Since the aperture of the receiver is diffraction limited the receiver aperture is dependent on the chosen instantaneous field of view. The receiver aperture diameter is then given by

$$D_R = .6 \frac{\lambda}{IFOV}$$

where the IFOV is given by the e^{-1} point of the diffraction pattern at the focal plane. For an IFOV of .1 mrad we have a required aperture diameter of 6.4 cm. If an investigation using a focal plane array is desired, it would be preferable to employ as small an IFOV as possible without being distrubed at atmospheric turbulence. A practical upper limit for a receiver aperture diameter is 15 cm for ranges of a few kilometers. If long range measurements are desired, it would be advisable to keep the maximum aperture to no more than 15 cm or 20 cm.

The transmitter aperture should be separate from the receiver so spatial correlation measurements can be conducted. Moreover, the distance between the transmitter and receiver aperture should not be fixed and a maximum separation of 30 cm should be possible. Note that a boresight alignment fixture will be required since a separated receiver and transmitter must be tilted with respect to another if they are to observe the same target.

To be able to change the target illumination diameter it will be necessary to have a transmitter with a variable beam divergence. This could be accomplished by having a variety of beam expanders available.

These beam expanders should mount to the instrument frame in a fashion that will allow a continual boresight adjustment with the receiver. The beam divergence capability should vary from .1 IFOV to 10 IFOV (IFOV refers to the receiver's instantaneous field of view).

Experiments involving specular targets will require that the receiver be capable of receiving signals at least 10^4 times the quantum noise limit. Moreover, the system response over this dynamic range should be linear to within 10%. If experiments are carried out at close ranges where the average signal is high, then the system should have neutral density filters available. The neutral density filters should be capable of an attenuation of 10^{-6} with grades of 10^{-1}.

The test system will be required to perform imaging as well as moving target indication. The MTI minimum resolvable velocity difference is given by

$$\delta v = \frac{f_D \lambda}{2}$$

where f_D is the doppler bandwidth. For δv = 3m/sec, we obtain a doppler bandwidth of $.6 \times 10^6$ Hz which gives a detector dwell time of

$$t_d = \frac{1}{2f_D} = .8 \times 10^{-6} \text{ sec.}$$

REFERENCES

1. M. Born and E. Wolf, Principles of Optics (MacMillan, New York, 1964), Chapter 10.

2. J. Goodman, Opt. Commun. 13, 244 (1975); see also Proc. IEEE 53 1968 (1965).

3. G. A. Cambell and R. M. Foster, Fourier Integrals for Practical Applications (Van Nostrand, Princeton, New Jersey, 1948).

4. C. W. Helstrom, Statistical Theory of Signal Detection (Pergamon Press, Oxford, 1968), 2nd Edition.

5. J. I. Marcum, "A Statistical Theory of Target Detection by Pulsed Radar," Report RM-753, Rand Corporation (1948).

6. S. O. Rice, "The Mathematical Analysis of Random Noise," Bell Syst. Tech. J. 23, 282-332 (1944); 24, 46-156 (1945). Reprinted in Noise and Stochastic Processes, N. Wax, Ed. (Dover Publications, New York, 1954).

7. J. I. Lawson and G. E. Uhlenbeck, Threshold Signals, M.I.T. Radiation Lab. Series, Vol. 24 (McGraw-Hill, New York, 1950).

8. R. Barakat, Opt. Commun. 8, 14 (1973).

9. D. L. Fried, Optical Science Consultants Reports: TR109 (1973), TR110 (1973), TR-116 (1973).

10. N. George and A. Jain, SPIE Proc., Vol. 41 (1973), p. 161.

UNCLASSIFIED

SECURITY CLASSIFICATION OF THIS PAGE *(When Data Entered)*

REPORT DOCUMENTATION PAGE	READ INSTRUCTIONS BEFORE COMPLETING FORM
1. REPORT NUMBER: ESD-TR-76-63	2. GOVT ACCESSION NO. / 3. RECIPIENT'S CATALOG NUMBER
4. TITLE *(and Subtitle)*: Diffuse Target Scintillation in 10.6 μm Laser Radar (Micrometers)	5. TYPE OF REPORT & PERIOD COVERED: Project Report / 6. PERFORMING ORG. REPORT NUMBER: Project Report TT-9
7. AUTHOR(s): Steven P. Tomczak	8. CONTRACT OR GRANT NUMBER(s): F19628-76-C-0002 / ARPA Order-2752
9. PERFORMING ORGANIZATION NAME AND ADDRESS: Lincoln Laboratory, M.I.T. P.O. Box 73 Lexington, MA 02173	10. PROGRAM ELEMENT, PROJECT, TASK AREA & WORK UNIT NUMBERS: ARPA Order 2752 Program Element No. 62702E Project No. 6G10
11. CONTROLLING OFFICE NAME AND ADDRESS: Defense Advanced Research Projects Agency 1400 Wilson Boulevard Arlington, VA 22209	12. REPORT DATE: 8 March 1976 / 13. NUMBER OF PAGES: 76
14. MONITORING AGENCY NAME & ADDRESS *(if different from Controlling Office)*: Electronic Systems Division Hanscom AFB Bedford, MA 01731 (12) 76p.	15. SECURITY CLASS. *(of this report)*: Unclassified / 15a. DECLASSIFICATION DOWNGRADING SCHEDULE
16. DISTRIBUTION STATEMENT *(of this Report)*: Approved for public release; distribution unlimited. (14) TT-9	
17. DISTRIBUTION STATEMENT *(of the abstract entered in Block 20, if different from Report)*	
18. SUPPLEMENTARY NOTES: None	
19. KEY WORDS *(Continue on reverse side if necessary and identify by block number)*: diffuse target scintillation; laser radar; heterodyne receiver; HOWLS Program; line scan systems	
20. ABSTRACT *(Continue on reverse side if necessary and identify by block number)*: This study is concerned with effects of diffuse target scintillation on 10.6 μm (micrometers) heterodyne line scan systems where the objective was to identify the problem areas which would eventually control the limiting factors in the image and MTI performance of line scan systems. In particular, diffuse target scintillation (speckle) was recognized as one of the limiting factors for a heterodyne receiver design and this study is concerned with the statistics of speckle noise and with speckle reduction techniques.	

DD FORM 1 JAN 73 1473 EDITION OF 1 NOV 65 IS OBSOLETE

UNCLASSIFIED

SECURITY CLASSIFICATION OF THIS PAGE *(When Data Entered)*